Standard and non-standard CAGD tools in Isogeometric Analysis

Carla Manni and Hendrik Speleers

Abstract We present a short summary of CAGD tools of main interest in IgA.

1 Bézier-Bernstein representations in 1D

1.1 Bernstein polynomials

Bernstein polynomials of degree p are defined as follows

$$B_i^{(p)}(t) := \binom{p}{i} t^i (1-t)^{p-i}, \qquad i = 0, \dots, p. \tag{1}$$

They form a basis for the space $\mathbb{P}_p$ of algebraic polynomials of degree p. Assuming $t \in [0,1]$[1], they possess the following interesting properties.

- *Positivity:*

$$B_i^{(p)}(t) \geq 0, \quad t \in [0,1]. \tag{2}$$

- *Partition of unity:*

$$\sum_{i=0}^{p} B_i^{(p)}(t) = (t+1-t)^p = 1, \quad \forall t \in \mathbb{R}. \tag{3}$$

Carla Manni
Dipartimento di Matematica, Università di Roma "Tor Vergata" - Italy
e-mail: manni@mat.uniroma2.it

Hendrik Speleers
Departement Computerwetenschappen, Katholieke Universiteit Leuven - Belgium
e-mail: hendrik.speleers@cs.kuleuven.be

[1] By the usual change of variable $t = \frac{x-a}{b-a}$, Bernstein polynomials can be considered on a general interval $[a,b]$.

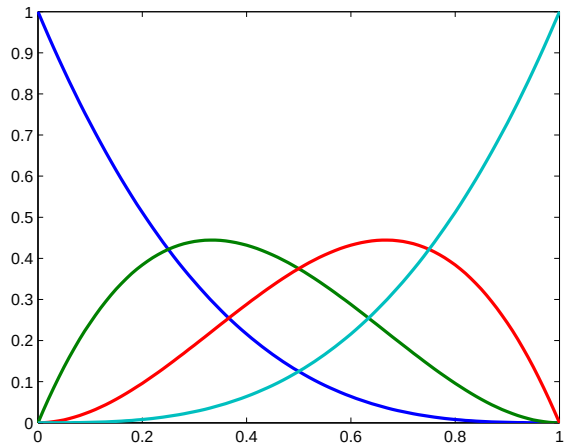

Fig. 1 Cubic Bernstein polynomials.

- *Recurrence relation:*

$$B_i^{(p)}(t) = (1-t)B_i^{(p-1)}(t) + tB_{i-1}^{(p-1)}(t), \tag{4}$$

  with $B_i^{(k)} = 0$ if $i < 0$ or $i > k$.
- *Degree raising/degree elevation:* since $\mathbb{P}_p \subset \mathbb{P}_{p+1}$,

$$B_i^{(p)}(t) = (t+1-t)B_i^{(p)}(t) = \frac{i+1}{p+1}B_{i+1}^{(p+1)}(t) + \frac{p+1-i}{p+1}B_i^{(p+1)}(t). \tag{5}$$

- *Integration:*

$$\int_0^1 B_i^{(p)}(t)\mathrm{d}t = \frac{1}{p+1}. \tag{6}$$

- *Derivatives:*
  - first derivative:

$$\frac{\mathrm{d}B_i^{(p)}(t)}{\mathrm{d}t} = p[B_{i-1}^{(p-1)}(t) - B_i^{(p-1)}(t)]; \tag{7}$$

  - end derivatives:

$$\frac{\mathrm{d}^r B_i^{(p)}(0)}{\mathrm{d}t^r} = 0, \quad r = 0,\ldots,i-1; \tag{8}$$

$$\frac{\mathrm{d}^r B_i^{(p)}(1)}{\mathrm{d}t^r} = 0, \quad r = 0,\ldots,p-i-1; \tag{9}$$

– unimodal behavior:

$$\frac{\mathrm{d}B_i^{(p)}(t)}{\mathrm{d}t} = 0, \quad \text{iff } t = \frac{i}{p},\ i = 1,\dots,p-1. \tag{10}$$

Example 1. By combining (6)–(8), and by setting

$$\delta_i^{(p)} := \frac{1}{\int_0^1 B_i^{(p)}(s)\mathrm{d}s},$$

we obtain the integral recurrence relation

$$\begin{aligned} B_0^{(p)}(t) &= 1 - \delta_0^{(p-1)} \int_0^t B_0^{(p-1)}(s)\mathrm{d}s, \\ B_i^{(p)}(t) &= \delta_{i-1}^{(p-1)} \int_0^t B_{i-1}^{(p-1)}(s)\mathrm{d}s - \delta_i^{(p-1)} \int_0^t B_i^{(p-1)}(s)\mathrm{d}s, \quad i = 1,\dots,p-1, \\ B_p^{(p)}(t) &= \delta_{p-1}^{(p-1)} \int_0^t B_{p-1}^{(p-1)}(s)\mathrm{d}s. \end{aligned} \tag{11}$$

Example 2. It can be easily seen by induction on $p \geq 1$ that

$$t = \sum_{i=0}^{p} \frac{i}{p} B_i^{(p)}(t). \tag{12}$$

The values $\xi_i^* := \frac{i}{p}$ are called **Greville abscissas**.

The previous properties have a number of fundamental geometric consequences. Let $\mathbf{P}_i \in \mathbb{R}^d$, $i = 0,\dots,p$, be given. The parametric curve

$$\mathcal{C}(t) := \sum_{i=0}^{p} \mathbf{P}_i B_i^{(p)}(t)$$

is called a **Bézier curve** in $\mathbb{R}^d$, the points $\mathbf{P}_i$ are their **control points**, and the polygon they form is referred to as **control polygon** of $\mathcal{C}$. The graph of any polynomial $q(t) = \sum_{i=0}^{p} q_i B_i^{(p)}(t)$ of degree p can be seen as a Bézier curve

$$\begin{pmatrix} t \\ q(t) \end{pmatrix} = \sum_{i=0}^{p} \begin{pmatrix} \xi_i^* \\ q_i \end{pmatrix} B_i^{(p)}(t),$$

and the polygonal line connecting $\begin{pmatrix} \xi_i^* \\ q_i \end{pmatrix}$, $i = 0,\dots,p$, is its control polygon.

- The partition of unity implies **affine invariance**:

$$\mathbf{P}_i \in \mathbb{R}^d,\ \mathcal{C}(t) = \sum_{i=0}^{p} \mathbf{P}_i B_i^{(p)}(t) \Rightarrow A\mathcal{C}(t) + \mathbf{Q} = \sum_{i=0}^{p} (A\mathbf{P}_i + \mathbf{Q}) B_i^{(p)}(t). \tag{13}$$

- The positivity and partition of unity provide the **convex hull** property:

$$\mathcal{C}(t) = \sum_{i=0}^{p} \mathbf{P}_i B_i^{(p)}(t) \in \mathcal{H}(\mathbf{P}_0, \ldots, \mathbf{P}_p). \tag{14}$$

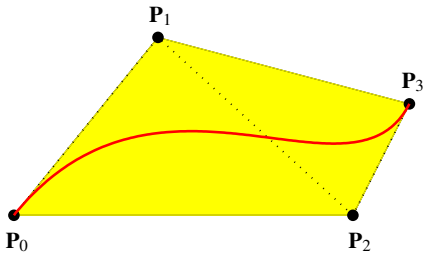

Fig. 2 Convex hull property for a cubic planar curve.

- The recurrence relation (4) leads to a stable evaluation algorithm:

$$\begin{aligned}\mathcal{C}(t) &= \sum_{i=0}^{p} \mathbf{P}_i^{[p]} B_i^{(p)}(t) \\ &= \sum_{i=0}^{p} \mathbf{P}_i^{[p]} [(1-t)B_i^{(p-1)}(t) + tB_{i-1}^{(p-1)}(t)] = \sum_{i=0}^{p-1} \mathbf{P}_i^{[p-1]} B_i^{(p-1)}(t) = \ldots = \mathbf{P}_0^{[0]},\end{aligned}$$

  with

$$\mathbf{P}_i^{[k-1]} := (1-t)\mathbf{P}_i^{[k]} + t\mathbf{P}_{i+1}^{[k]}, \quad i = 0, \ldots, k-1. \tag{15}$$

  The previous algorithm is known as the **de Casteljau algorithm** and provides a very efficient tool to evaluate a Bézier curve at a given parameter value $t \in [0,1]$. The evaluation is numerically stable because it is based on convex combinations.
- By degree raising of the Bernstein polynomials (5), and by setting $\mathbf{P}_{-1} := 0$, $\mathbf{P}_{p+1} := 0$, we have

$$\sum_{i=0}^{p} \mathbf{P}_i B_i^{(p)}(t) = \sum_{i=0}^{p+1} \hat{\mathbf{P}}_i B_i^{(p+1)}(t), \quad \hat{\mathbf{P}}_i := \frac{p+1-i}{p+1}\mathbf{P}_i + \frac{i}{p+1}\mathbf{P}_{i-1}. \tag{16}$$

- Derivatives of Bézier curves are obtained by applying (7) inductively:

$$\frac{\mathrm{d}\mathcal{C}(t)}{\mathrm{d}t} = p \sum_{i=0}^{p-1} (\mathbf{P}_{i+1} - \mathbf{P}_i) B_i^{(p-1)}(t), \tag{17}$$

$$\frac{\mathrm{d}^r\mathcal{C}(t)}{\mathrm{d}t^r} = \frac{p!}{(p-r)!} \sum_{i=0}^{p-r} \Delta_r(\mathbf{P}_i) B_i^{(p-r)}(t), \tag{18}$$

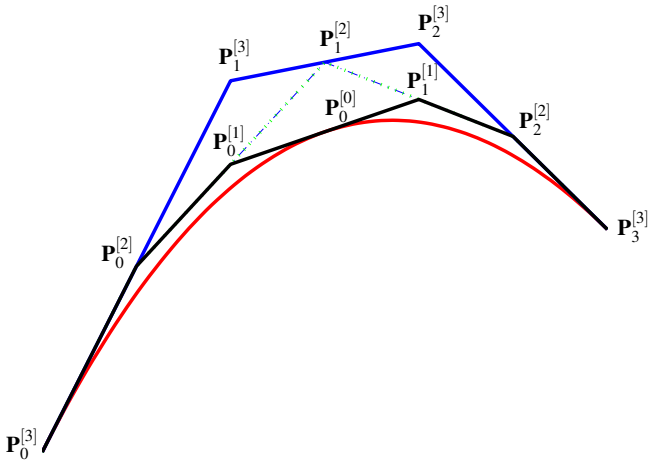

Fig. 3 The de Casteljau algorithm for a cubic Bézier curve.

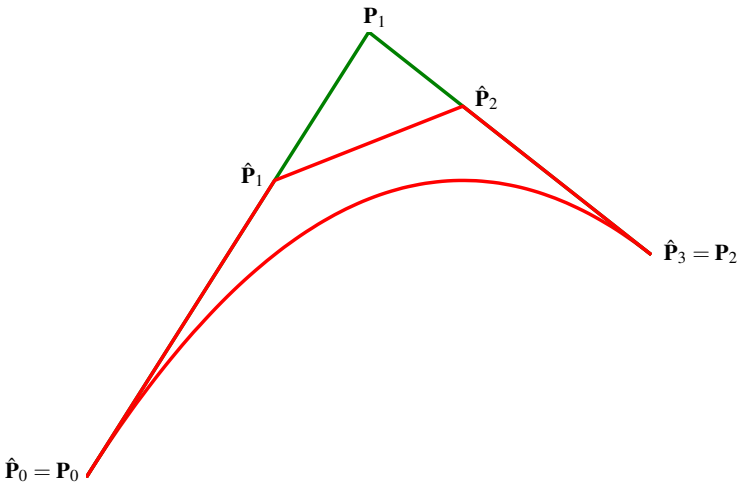

Fig. 4 Degree raising for a quadratic Bézier curve.

with

$$\Delta_r(\mathbf{P}_i) := \sum_{k=0}^{r} \binom{r}{k} (-1)^{r-k} \mathbf{P}_{i+k}.$$

Only $r+1$ control points are involved in the expression for the r-th order derivative evaluated at the two endpoints. Moreover, (17) implies that the control polygon is tangent to the curve at both end points.

- C^r continuity of two adjacent Bézier curves

$$\sum_{j=0}^{p} \mathbf{P}_j^L B_j^{(p)}(t), \quad \sum_{j=0}^{p} \mathbf{P}_j^R B_j^{(p)}(t)$$

has a simple geometric interpretation thanks to the local behavior of the derivatives at the end points, see (17) and (18). In particular, C^0 continuity just requires that $\mathbf{P}_p^L = \mathbf{P}_0^R$, while C^1 continuity implies, in addition, that the two segments $\mathbf{P}_{p-1}^L \mathbf{P}_p^L$ and $\mathbf{P}_0^R \mathbf{P}_1^R$ are collinear, see Figure 5 (right).

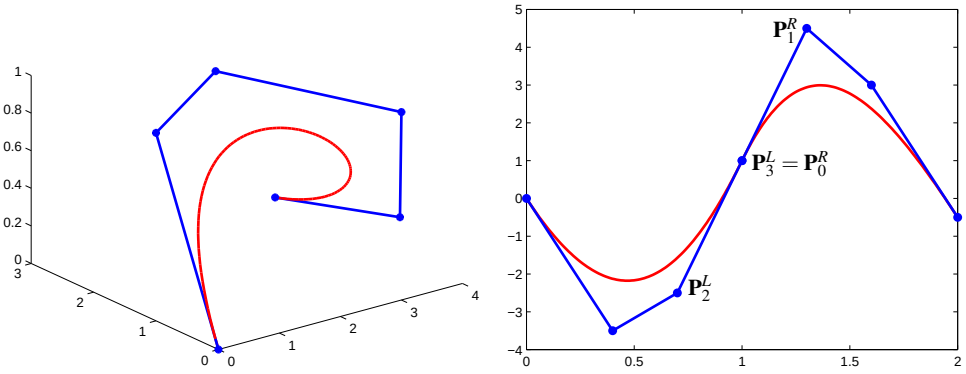

Fig. 5 Left: a quintic Bézier curve and its control polygon. Right: C^1 joint between two cubic Bézier curves.

1.2 Total positivity

Definition 1. A matrix is **totally positive (TP)** if any subdeterminant is ≥ 0.

Definition 2. A basis $\{\varphi_0, \ldots, \varphi_p\}$ of a space $\mathbb{U}_p$ is **totally positive** in $I \subset \mathbb{R}$ if any collocation matrix

$$\begin{pmatrix} \varphi_0(t_1) & \ldots & \varphi_p(t_1) \\ \vdots & & \vdots \\ \varphi_0(t_r) & \ldots & \varphi_p(t_r) \end{pmatrix} \tag{19}$$

$$t_1 < t_2 < \ldots < t_r, \quad t_i \in I,\ i = 1, \ldots, r,$$

is TP.

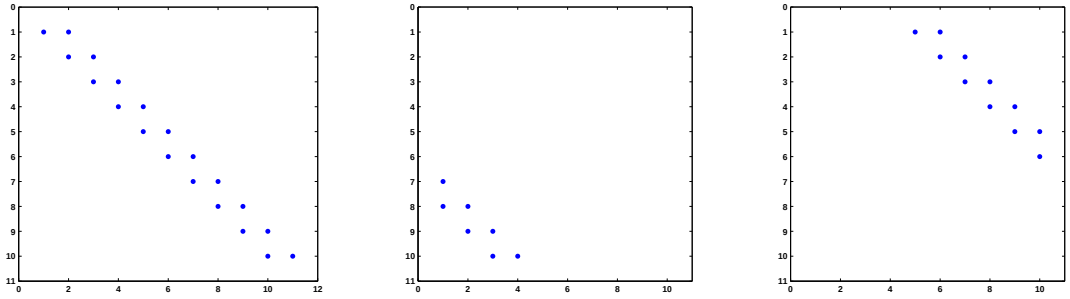

Fig. 6 Bidiagonal matrices.

Definition 3. A matrix is **stochastic** if it is positive and the entries in each row sum up to one.

Theorem 1. *Any positive "bidiagonal matrix" is TP.*

Theorem 2. *A matrix is (stochastic) TP iff it is the product of (stochastic) positive "bidiagonal" matrices.*

Corollary 1. *If $\{\varphi_0,\dots,\varphi_p\}$ is a TP basis and $c_0,\dots,c_p \in \mathbb{R}$, then the number of sign changes of $(\sum_{i=0}^{p} c_i\varphi_i(t))$ is less than or equal to the number of sign changes of $(c_0,\dots,c_p)$.*

Definition 4. A basis $\{\varphi_0,\dots,\varphi_p\}$ is **normalized** if $\sum_{j=0}^{p}\varphi_j = 1$.

Proposition 1 (Variation diminishing). *Let $\{\varphi_0,\dots,\varphi_p\}$ be a normalized TP basis. Define the planar curve $\mathcal{C}(t) = \sum_{j=0}^{p}\mathbf{C}_j\varphi_j(t)$, $t \in I$, $\mathbf{C}_j \in \mathbb{R}^2$. Then the number of times $\mathcal{C}$ crosses any straight line ℓ is bounded by the number of times the control polygon $\mathbf{C}_0\dots\mathbf{C}_p$ crosses ℓ.*

The previous result ensures that TP bases provide shape-preserving representations.

Lemma 1 (Fekete). *A matrix is strictly TP iff any square submatrix consisting of consecutive rows/columns is strictly TP.*

Example 3. The monomial basis $\{1,t,\dots,t^p\}$ is TP in $[0,+\infty)$.

Proposition 2. *Let $\{\varphi_0,\dots,\varphi_p\}$ be TP in I.*

- *if $f : J \to I$ is increasing then $\{\varphi_0\circ f,\dots,\varphi_p\circ f\}$ is TP in J;*
- *if g is nonnegative in I then $\{g\varphi_0,\dots,g\varphi_p\}$ is TP in I;*
- *if $A := (a_{ij})$ is a TP matrix then $\{\sum_{j=0}^{p} a_{0j}\varphi_j,\dots,\sum_{j=0}^{p} a_{pj}\varphi_j\}$ is TP in I.*

Example 4. The Bernstein basis is TP in $[0,1]$.

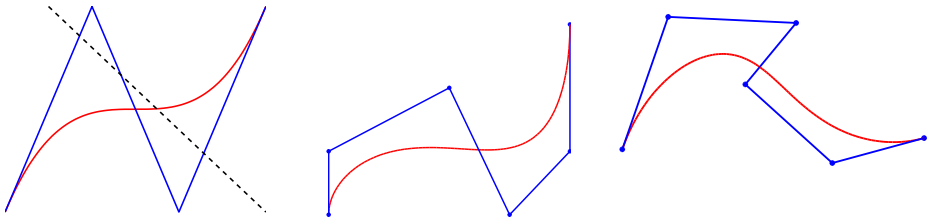

Fig. 7 Variation diminishing.

Theorem 3 ([10]). *Suppose that the space $\mathbb{U}_p$ possesses a normalized TP (NTP) basis. Then it possesses a unique NTP basis $(\vartheta_0,\dots,\vartheta_p)$ such that any other NTP basis $(\varphi_0,\dots,\varphi_p)$ is given by*

$$(\varphi_0,\dots,\varphi_p) = (\vartheta_0,\dots,\vartheta_p)K,$$

where the matrix K is stochastic and TP. We then say that $(\vartheta_0,\dots,\vartheta_p)$ is the optimal NTP basis (in short, the ONTP basis) of the space $\mathbb{U}_p$.

Theorem 4. *A nonsingular stochastic TP matrix can be decomposed as the product of matrices of the form*

$$\begin{pmatrix} 1 & 0 & 0 & \cdots & \cdots & 0 \\ 0 & 1 & 0 & \cdots & \cdots & 0 \\ & \ddots & & & & \\ 0 & & 1-\lambda_i & \lambda_i & & 0 \\ 0 & & 0 & 1 & & 0 \\ & & & & \ddots & 0 \\ 0 & 0 & \cdots & \cdots & 0 & 1 \end{pmatrix}, \quad \begin{pmatrix} 1 & 0 & 0 & \cdots & \cdots & 0 \\ 0 & 1 & 0 & \cdots & \cdots & 0 \\ & \ddots & & & & \\ 0 & & 1 & 0 & & 0 \\ 0 & & \mu_i & 1-\mu_i & & 0 \\ & & & & \ddots & 0 \\ 0 & 0 & \cdots & \cdots & 0 & 1 \end{pmatrix}, \quad \lambda_i,\ \mu_i \in [0,1)$$

Example 5. The local effect of such a matrix is illustrated by

$$\begin{pmatrix} 1 & 0 & 0 & \cdots & \cdots & 0 \\ 0 & 1 & 0 & \cdots & \cdots & 0 \\ & \ddots & & & & \\ 0 & & 1-\lambda_i & \lambda_i & & 0 \\ 0 & & 0 & 1 & & 0 \\ & & & & \ddots & 0 \\ 0 & 0 & \cdots & \cdots & 0 & 1 \end{pmatrix} \begin{pmatrix} \mathbf{Q}_0 \\ \mathbf{Q}_1 \\ \\ \\ \vdots \\ \\ \mathbf{Q}_p \end{pmatrix} = \begin{pmatrix} \mathbf{Q}_0 \\ \mathbf{Q}_1 \\ \\ (1-\lambda_i)\mathbf{Q}_i + \lambda_i \mathbf{Q}_{i+1} \\ \vdots \\ \\ \mathbf{Q}_p \end{pmatrix}.$$

Let $\{\vartheta_0,\dots,\vartheta_p\}$ be the ONTP basis for $\mathbb{U}_p$, and $\{\varphi_0,\dots,\varphi_p\}$ be an NTP basis, and

$$\mathcal{C}(t) := \sum_{j=0}^{p} \mathbf{Q}_j \varphi_j(t) = \sum_{j=0}^{p} \mathbf{Q}_j \sum_{i=0}^{p} k_{ij} \vartheta_i(t) = \sum_{i=0}^{p} \left(\sum_{j=0}^{p} k_{ij} \mathbf{Q}_j \right) \vartheta_i(t) = \sum_{i=0}^{p} \mathbf{P}_i \vartheta_i(t),$$

$$\begin{pmatrix} \mathbf{P}_0 \\ \vdots \\ \mathbf{P}_p \end{pmatrix} = K \begin{pmatrix} \mathbf{Q}_0 \\ \vdots \\ \mathbf{Q}_p \end{pmatrix}.$$

It follows that the control polygon of $\mathcal{C}$ with respect to the ONTP basis is obtained via corner cutting from the control polygon with respect to any other NTP basis. Hence, the control polygon representation with respect to the ONTP basis is the closest one to $\mathcal{C}$. It lies "between" and the control polygon with respect to any other NTP basis.

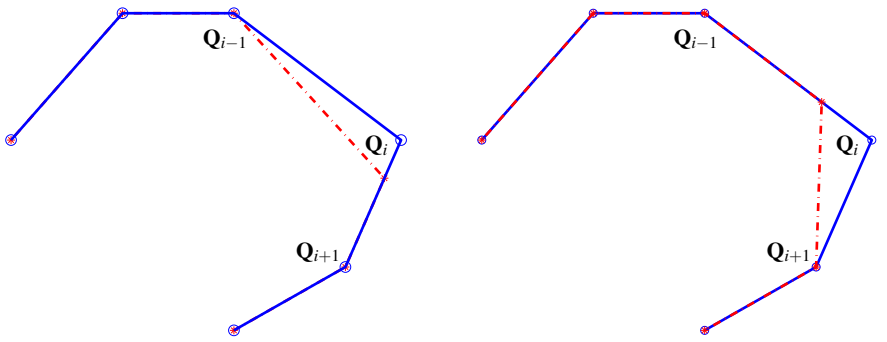

Fig. 8 Elementary corner cutting.

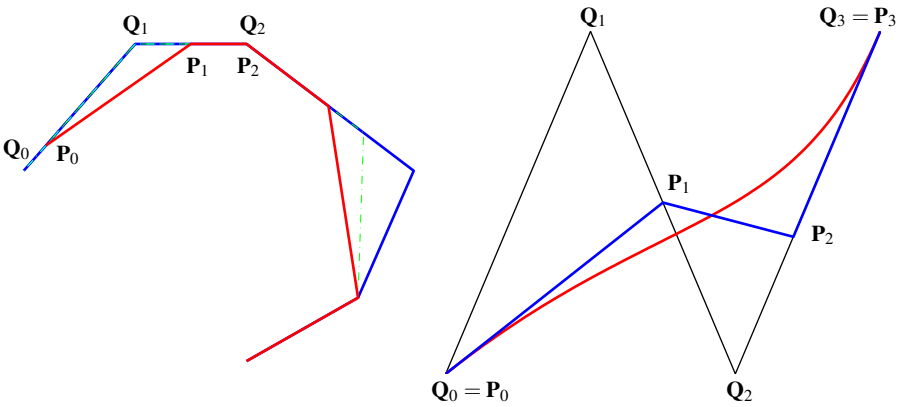

Fig. 9 Corner cutting.

Theorem 5 ([34], Proposition 3.2). *Suppose that the space $\mathbb{U}_p$ possesses an NTP basis and denote by $(\vartheta_0,\dots,\vartheta_p)$ the ONTP one. Then,*

- *for $i=0,\dots,p$, the set $I_i := \{x\in I:\ \vartheta_i(x)\neq 0\}$ is an interval;*
- *setting $a_i := \inf I_i$, $b_i := \sup I_i$, for $0\le i\le p$, we have, for $k<i$,*

$$a_k \le a_i,\ b_k \le b_i, \quad \lim_{x\to a_k^+}\frac{\vartheta_i(x)}{\vartheta_k(x)}=0,\ \lim_{x\to b_i^-}\frac{\vartheta_k(x)}{\vartheta_i(x)}=0. \tag{20}$$

Corollary 2. *Bernstein polynomials are the ONTP basis of $\mathbb{P}_p$ in $[0,1]$.*

2 Piecewise spaces: B-splines

Let a sequence of knots be given

$$\Xi := \{\xi_1\le\xi_2\le\ldots\le\xi_{n+p+1}\}, \tag{21}$$

we say that the knot ξ_i has multiplicity $1\le\rho_i\le p+1$ if

$$\ldots<\xi_i=\xi_{i+1}=\ldots=\xi_{i+\rho_i-1}<\xi_{i+\rho_i}.$$

Usually, one takes

$$\xi_1=\ldots=\xi_{p+1}<\ldots<\xi_{n+1}=\ldots=\xi_{n+p+1}.$$

The B-splines of degree p, related to the knots Ξ, are defined by

$$\begin{aligned} B_{i,\Xi}^{(0)}(t) &:= \begin{cases} 1, & \text{if } t\in[\xi_i,\xi_{i+1}),\\ 0, & \text{elsewhere,}\end{cases}\\ B_{i,\Xi}^{(p)}(t) &:= \frac{t-\xi_i}{\xi_{i+p}-\xi_i}B_{i,\Xi}^{(p-1)}(t)+\frac{\xi_{i+p+1}-t}{\xi_{i+p+1}-\xi_{i+1}}B_{i+1,\Xi}^{(p-1)}(t), \quad p\ge 1. \end{aligned} \tag{22}$$

In the following we denote

$$\mathbb{S}_{p,\Xi} := \left\{\sum_j c_j B_{j,\Xi}^{(p)}\right\}.$$

2.1 Evaluation and related properties

By setting

$$\omega_{i,p}(t) := \frac{t-\xi_i}{\xi_{i+p}-\xi_i},$$

we have

$$B_{i,\Xi}^{(p)}(t) = \omega_{i,p}(t)B_{i,\Xi}^{(p-1)}(t) + (1-\omega_{i+1,p}(t))B_{i+1,\Xi}^{(p-1)}(t).$$

Therefore, the spline curve

$$\mathcal{C}(t) := \sum_i \mathbf{C}_i^{[p]} B_{i,\Xi}^{(p)}(t), \quad t \in [\xi_r, \xi_{r+1}),$$

can be written as

$$\begin{aligned}\sum_i \mathbf{C}_i^{[p]} B_{i,\Xi}^{(p)}(t) &= \sum_i \mathbf{C}_i^{[p]} [\omega_{i,p}(t)B_{i,\Xi}^{(p-1)}(t) + (1-\omega_{i+1,p}(t))B_{i+1,\Xi}^{(p-1)}(t)] \\ &= \sum_j \mathbf{C}_j^{[p-1]} B_{j,\Xi}^{(p-1)}(t) = \ldots = \sum_j \mathbf{C}_j^{[0]} B_{j,\Xi}^{(0)}(t) = \mathbf{C}_r^{[0]},\end{aligned}$$

where at each step the new coefficients are obtained by a convex combination, actually

$$\mathbf{C}_i^{[k-1]} := \omega_{i,k}(t)\mathbf{C}_i^{[k]} + (1-\omega_{i,k}(t))\mathbf{C}_{i-1}^{[k]}, \quad k = p, p-1, ..., 1. \tag{23}$$

This evaluation procedure is known as the **de Boor Algorithm**.

From the previous evaluation procedure we immediately obtain the following properties.

- *Piecewise polynomials:* $B_{i,\Xi}^{(p)}(t) \in \mathbb{P}_p, t \in [\xi_j, \xi_{j+1})$.
- *Positivity:* $B_{i,\Xi}^{(p)} \geq 0$.
- *Compact (minimum) support:*

$$\begin{aligned}&B_{i,\Xi}^{(p)}(t) = 0, \quad t \notin [\xi_i, \xi_{i+p+1}], \\ &B_{i,\Xi}^{(p)}(t) = 0, \quad t \in [\xi_r, \xi_{r+1}),\ i \notin \{r, r-1, .., r-p\}.\end{aligned}$$

Example 6. Considering the sequence of knots

$$\Xi := \{0 = \xi_0 = \ldots = \xi_p < \xi_{p+1} = \ldots = \xi_{p+p+1} = 1\}$$

we have $B_{i,\Xi}^{(p)}(t) = B_i^{(p)}(t)$ i.e. the Bernstein polynomials.

2.2 Polynomials in $\mathbb{S}_{p,\Xi}$

Let

$$\psi_{i,0}(\tau) := 1, \quad \psi_{i,p}(\tau) := (\xi_{i+1} - \tau)\ldots(\xi_{i+p} - \tau). \tag{24}$$

Proposition 3.

$$\frac{(t-\tau)^{p-\nu}}{(p-\nu)!} = \sum_i \frac{(-1)^\nu}{p!} \frac{\mathrm{d}^\nu \psi_{i,p}(\tau)}{\mathrm{d}\tau^\nu} B_{i,\Xi}^{(p)}(t), \quad t \in [\xi_{p+1}, \xi_{n+1}), \quad 0 \leq \nu \leq p. \tag{25}$$

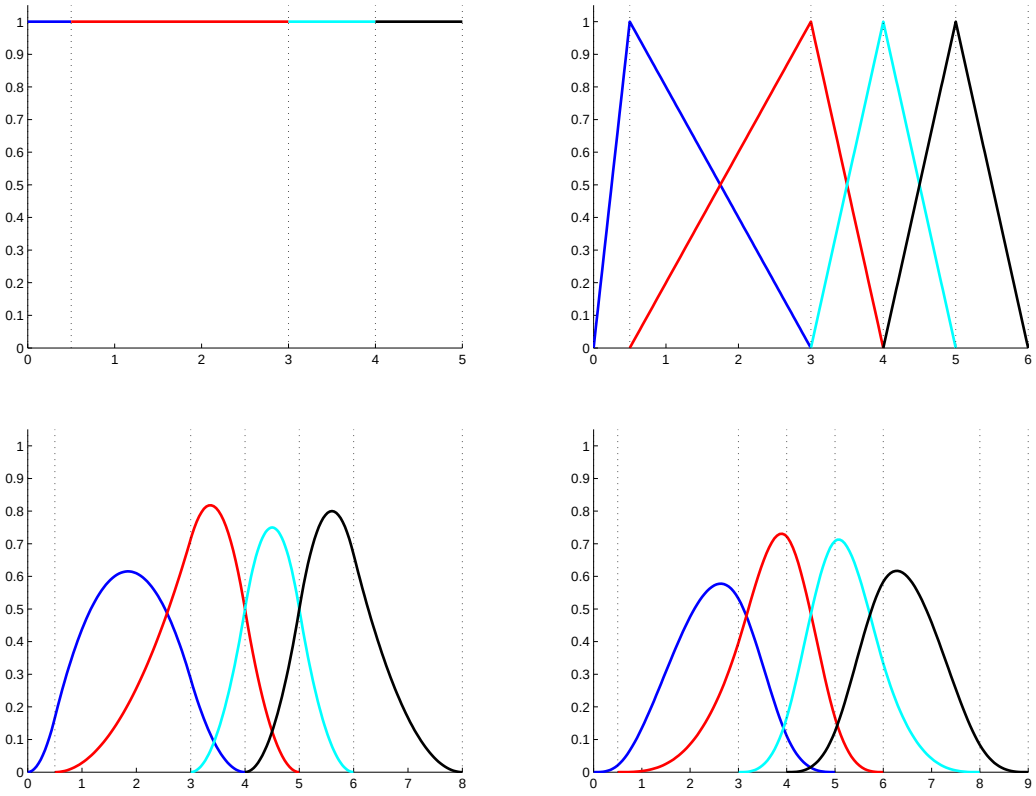

Fig. 10 B-splines of degree 0, 1, 2 and 3.

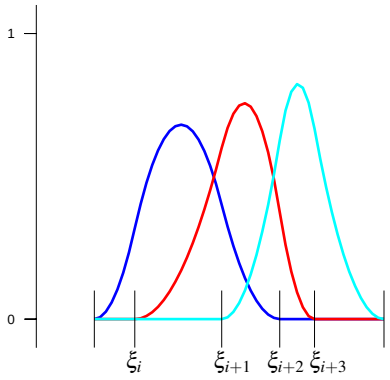

Fig. 11 Compact support of B-splines of degree 2.

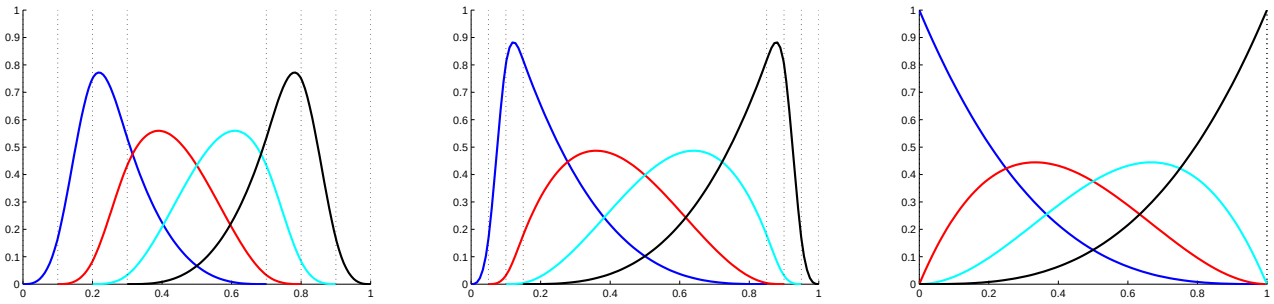

Fig. 12 B-splines of degree 3 over particular sequences of knots. In the three pictures 4 knots are moving towards the left as well as towards the right end of the interval $[0,1]$.

Proof.

$$\omega_{i,p}\psi_{i,p}(\tau)+(1-\omega_{i,p})\psi_{i-1,p}=(t-\tau)\psi_{i,p-1}(\tau),$$

therefore

$$\begin{aligned}\sum_i \psi_{i,p}(\tau)B_{i,\Xi}^{(p)}(t) &= \sum_i \psi_{i,p}(\tau)[(\omega_{i,p}(t)B_{i,\Xi}^{(p-1)}(t)+(1-\omega_{i+1,p}(t))B_{i+1,\Xi}^{(p-1)}(t)]\\ &= \sum_i [\omega_{i,p}\psi_{i,p}(\tau)+(1-\omega_{i,p})\psi_{i-1,p}]B_{i,\Xi}^{(p-1)}(t)\\ &= (t-\tau)\sum_i \psi_{i,p-1}(\tau)B_{i,\Xi}^{(p-1)}(t)=\ldots=(t-\tau)^p\sum_i \psi_{i,0}(\tau)B_{i,\Xi}^{(0)}(t).\end{aligned}$$

The assertion follows after dividing by $p!$ and after deriving ν times with respect to τ. □

- *Marsden's identity:* formula (25) and Taylor expansion give

$$q(t)=\sum_{i=1}^{n}\Lambda_{i,p}(q)B_{i,\Xi}^{(p)}(t),\quad \forall q\in\mathbb{P}_p,\quad t\in[\xi_{p+1},\xi_{n+1}),\tag{26}$$

  where

$$\Lambda_{i,p}(q):=\sum_{r=0}^{p}\frac{(-1)^r}{p!}\frac{\mathrm{d}^r\psi_{i,p}(\tau)}{\mathrm{d}\tau^r}\frac{\mathrm{d}^{p-r}q(\tau)}{\mathrm{d}t^{p-r}}.$$

- *(Local) partition of unity:* considering $q(t)=1$,

$$1=\sum_{i=1}^{n}B_{i,\Xi}^{(p)}(t),\quad t\in[\xi_{p+1},\xi_{n+1}),$$

$$1=\sum_{r=i-p}^{i}B_{r,\Xi}^{(p)}(t),\quad t\in[\xi_i,\xi_{i+1}).$$

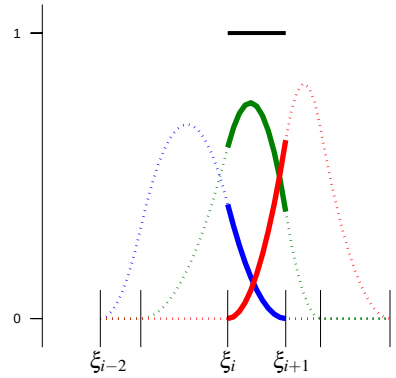

Fig. 13 Local partition of unity.

- *Greville abscissas:* considering $q(t) = t$,

$$\Lambda_{i,p}(q) = \frac{\xi_{i+1} + \ldots + \xi_{i+p}}{p} =: \xi_i^*;$$

$$t = \sum_{i=1}^{n} \xi_i^* B_{i,\Xi}^{(p)}(t), \quad t \in [\xi_{p+1}, \xi_{n+1}). \tag{27}$$

- *(Local) convex hull:* given $t \in [\xi_i,\ \xi_{i+1})$ and

$$\mathcal{C}(t) := \sum_{j=1}^{n} \mathbf{C}_j B_{j,\Xi}^{(p)}(t), \quad \mathbf{C}_j \in \mathbb{R}^d,$$

the positivity and (local) partition of unity imply that only $\mathbf{C}_{i-p}, \ldots \mathbf{C}_{i-1}, \mathbf{C}_i$ act on $\mathcal{C}(t)$, and that

$$\mathcal{C}(t) \in \mathcal{H}(\mathbf{C}_{i-p}, \ldots \mathbf{C}_{i-1}, \mathbf{C}_i).$$

In case of scalar functions

$$\begin{pmatrix} t \\ f(t) \end{pmatrix} = \sum_{j=1}^{n} \begin{pmatrix} \xi_j^* \\ c_j \end{pmatrix} B_{j,\Xi}^{(p)}(t),$$

and $t \in [\xi_i,\ \xi_{i+1})$, only $c_{i-p}, \ldots, c_{i-1}, c_i$, have an effect on $f(t)$.

The polygonal line connecting the points $\mathbf{C}_i \in \mathbb{R}^d$ (or the points $\begin{pmatrix} \xi_i^* \\ c_i \end{pmatrix}$ in the plane) is the **control polygon** of $\mathcal{C}$ (or f).

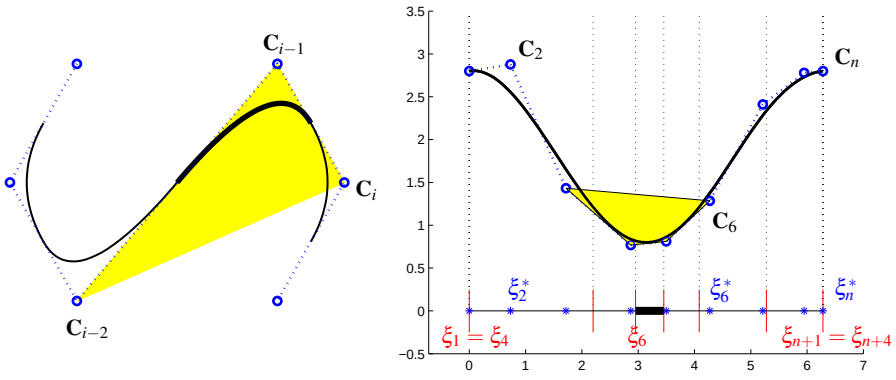

Fig. 14 Local convex hull for a quadratic curve (left) and a cubic spline function (right).

2.3 Knots multiplicity and truncated powers in $\mathbb{S}_{p,\Xi}$

The truncated power function is denoted by

$$(x)_+^r := (\max(x,0))^r.$$

We have, similarly to (25),

$$\frac{(t-\xi_k)_+^{p-\mu}}{(p-\mu)!} = \sum_{i\geq k} \frac{(-1)^\mu}{p!} \frac{\mathrm{d}^\mu \psi_{i,p}(\xi_k)}{\mathrm{d}\tau^\mu} B_{i,\Xi}^{(p)}(t), \quad t \in [\xi_{p+1}, \xi_{n+1}), \quad \forall\, 0 \leq \mu < \rho_k, \tag{28}$$

where we take the μ-th order derivative of $\psi_{i,p}(\tau)$, defined in (24), and evaluate it at the knot ξ_k. Therefore, polynomials of degree p and truncated powers of the form

$$(.-\xi_k)_+^{\nu_k}, \quad p-\rho_k < \nu_k \leq p$$

belong to $\mathbb{S}_{p,\Xi}$.

Given a set of (strictly increasing) break points

$$\hat{\Xi} := \{\hat{\xi}_0 < \hat{\xi}_1 < \ldots < \hat{\xi}_{l+1}\},$$

and the sequence of integers

$$\boldsymbol{\nu} := \{\nu_1, \ldots, \nu_l\},$$

the space of piecewise polynomials with given smoothness at the break points is defined by

$$\mathbb{P}_{p,\hat{\Xi}}^{\boldsymbol{\nu}} := \left\{ s : \; s_{|[\hat{\xi}_i, \hat{\xi}_{i+1})} \in \mathbb{P}_p, \; s^{(j)}(\hat{\xi}_i^+) = s^{(j)}(\hat{\xi}_i^-), \; j = 0, \ldots, \nu_i - 1, \; i = 1, \ldots, l \right\}.$$

It is easy to see that

$$\mathbb{P}^{\boldsymbol{\nu}}_{p,\hat{\Xi}} = \langle 1, t, \ldots, t^p, (t-\hat{\xi}_1)^{\nu_1}_+, \ldots, (t-\hat{\xi}_1)^p_+, \ldots, (t-\hat{\xi}_l)^{\nu_l}_+, \ldots, (t-\hat{\xi}_l)^p_+ \rangle.$$

This basically gives the following result.

Theorem 6 (Curry-Schoenberg, 1966). *Let*

$$\Xi := \{\xi_1 \le \xi_2 \le \ldots \le \xi_{n+p+1}\},$$

so that

- $\xi_1 \le \ldots \le \xi_{p+1} \le \hat{\xi}_0 < \ldots < \hat{\xi}_{l+1} \le \xi_{n+1} \le \ldots \le \xi_{n+p+1}$,
- $\hat{\xi}_j$ *occurs* $p+1-\nu_j$ *times in* Ξ, $j = 1, \ldots, l$,

then $\{B^{(p)}_{1,\Xi}, \ldots, B^{(p)}_{n,\Xi}\}$ *is a basis of* $\mathbb{P}^{\boldsymbol{\nu}}_{p,\hat{\Xi}}$ *in* $[\xi_{p+1}, \xi_{n+1})$.

Remark 1. At a given knot ξ_i of multiplicity $1 \le \rho_i \le p+1$, any element of $\mathbb{S}_{p,\Xi}$ is (at least) of class $C^{\nu_i - 1}$ where

$$p + 1 = \nu_i + \rho_i. \tag{29}$$

Corollary 3 (local linear independence). *In* $[\xi_r, \xi_{r+1})$ *we have*

$$\langle B^{(p)}_{r-p,\Xi}, \ldots, B^{(p)}_{r,\Xi} \rangle \equiv \mathbb{P}_{p\,|\,[\xi_r, \xi_{r+1})}.$$

Therefore in $[\xi_r, \xi_{r+1})$ *any element of* $\mathbb{S}_{p,\Xi}$ *can be represented as a linear combination of Bernstein polynomials.*

Corollary 4 (de Boor-Fix formula). *The elements of the space* $\mathbb{S}_{p,\Xi}$ *can be represented as*

$$f(t) = \sum_i \Lambda_{i,p}(f) B^{(p)}_{i,\Xi}(t), \quad \forall f \in \mathbb{S}_{p,\Xi}, \tag{30}$$

where

$$\Lambda_{i,p}(f) := \sum_{r=0}^{p} \frac{(-1)^r}{p!} \frac{\mathrm{d}^r \psi_{i,p}(\tau_i)}{\mathrm{d}\tau^r} \frac{\mathrm{d}^{p-r} f(\tau_i)}{\mathrm{d}t^{p-r}}, \quad \xi_i^+ \le \tau_i \le \xi_{i+p+1}^-.$$

2.4 Knot insertion

Let us consider

$$\Xi := \{\ldots \le \xi_i \le \xi_{i+1} \le \ldots\} \subset \{\ldots \le \xi_i \le \bar{\xi} \le \xi_{i+1} \le \ldots\} =: \bar{\Xi},$$

then $\mathbb{S}_{p,\Xi} \subset \mathbb{S}_{p,\bar{\Xi}}$, so that

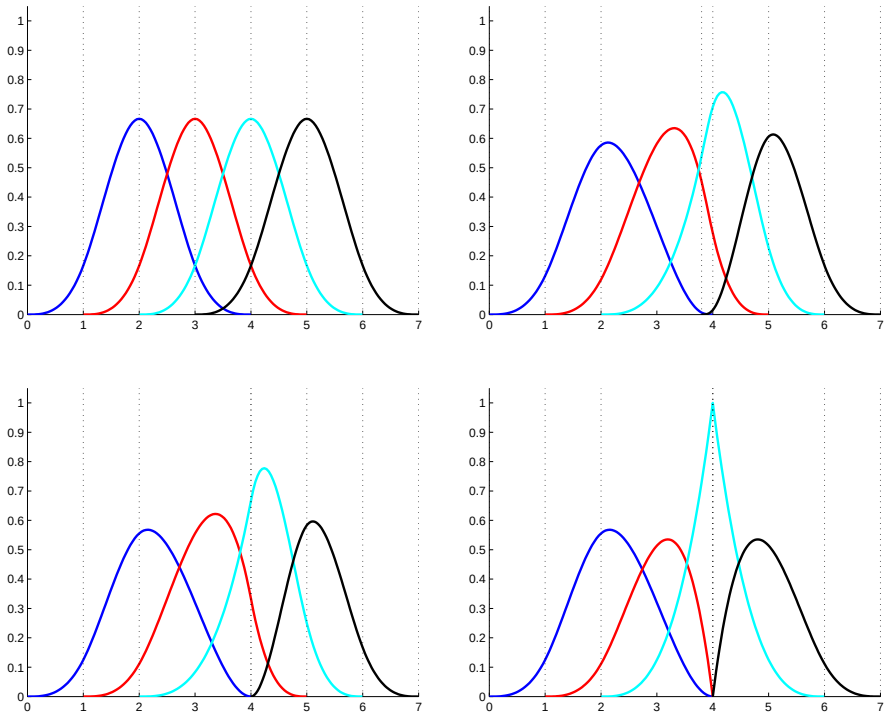

Fig. 15 Smoothness and knot multiplicity for cubic B-splines with different knot sequences $\Xi =$ [0, 1, 2, 3, 4, 5, 6, 7], [0, 1, 2, 3.9, 4, 5, 6, 7], [0, 1, 2, 4, 4, 5, 6, 7], [0, 1, 2, 4, 4, 4, 6, 7].

$$\sum_j \mathbf{C}_j B^{(p)}_{j,\Xi} = \sum_j \bar{\mathbf{C}}_j B^{(p)}_{j,\bar{\Xi}}. \tag{31}$$

From (30) we obtain

$$\bar{\mathbf{C}}_j = \bar{\omega}_{j,p}\mathbf{C}_j + (1-\bar{\omega}_{j,p})\mathbf{C}_{j-1}, \qquad \bar{\omega}_{j,p} := \begin{cases} 1, & \xi_{j+p} \le \bar{\xi}, \\ \frac{\bar{\xi}-\xi_j}{\xi_{j+p}-\xi_j}, & \xi_j < \bar{\xi} < \xi_{j+p}, \\ 0, & \bar{\xi} \le \xi_j, \end{cases} \tag{32}$$

Remark 2. The new control polygon interpolates the old one at the new Greville abscissas (corner cutting).

Remark 3. Note that (32) is nothing else than applying one step of the de Boor algorithm. Therefore, the de Boor algorithm can be seen as repeated corner cuttings.

Remark 4. When several knots have to be inserted at the same time, more efficient algorithms can be used instead of repeating (32), see for instance the Oslo algorithm [11].

Remark 5. The (single) knot insertion can be iterated. The finer the knot sequence, the closer is the control polygon to the function being represented. There is convergence under knot refinement. It corresponds to h-refinement in IgA.

Remark 6. A fast and elegant way to visualize spline curves is based on repeating knot insertion: after inserting a few times a knot between each pair of existing knots, it is sufficient to draw the control polygon. In the case of equally spaced knots, this procedure basically leads to classical subdivision schemes, see [14].

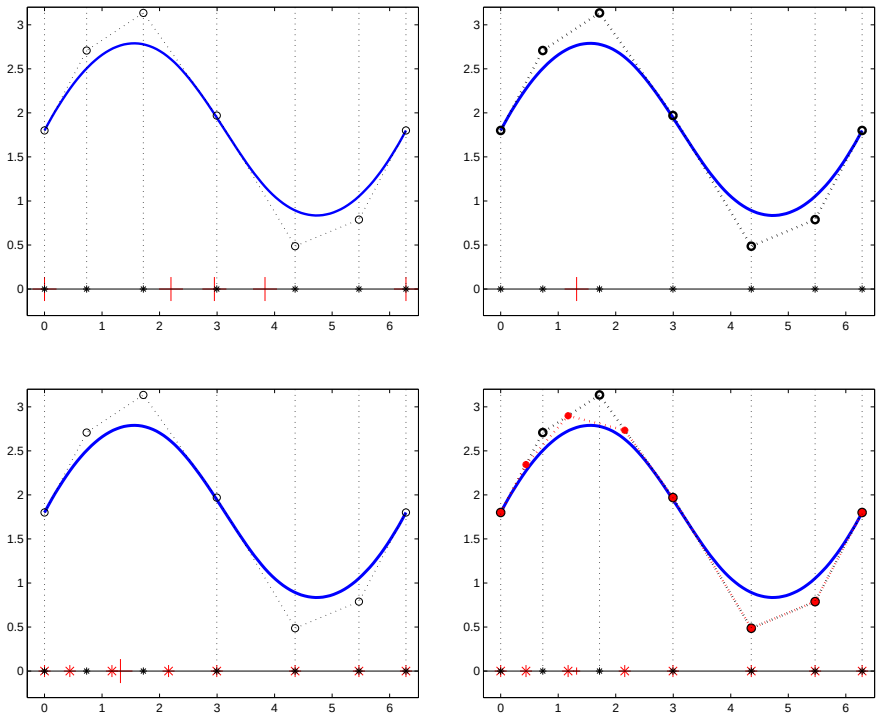

Fig. 16 Knot insertion for cubic B-splines.

From (32) it follows that the number of sign changes in the sequence $\{\ldots\bar{c}_j\ldots\}$ is bounded above by the number of sign changes in the sequence $\{\ldots c_j\ldots\}$.
Moreover, considering the repeated insertion of a point x, p times, so that for some r

$$\xi_r < \xi_{r+1} = \ldots = \xi_{r+p} = x < \xi_{r+p+1},$$

then $B^{(p)}_{j,\Xi}(x) = \delta_{r,j}$ so that

$$\sum_j c_j B^{(p)}_{j,\Xi}(x) = c_r B^{(p)}_{r,\Xi}(x) = c_r.$$

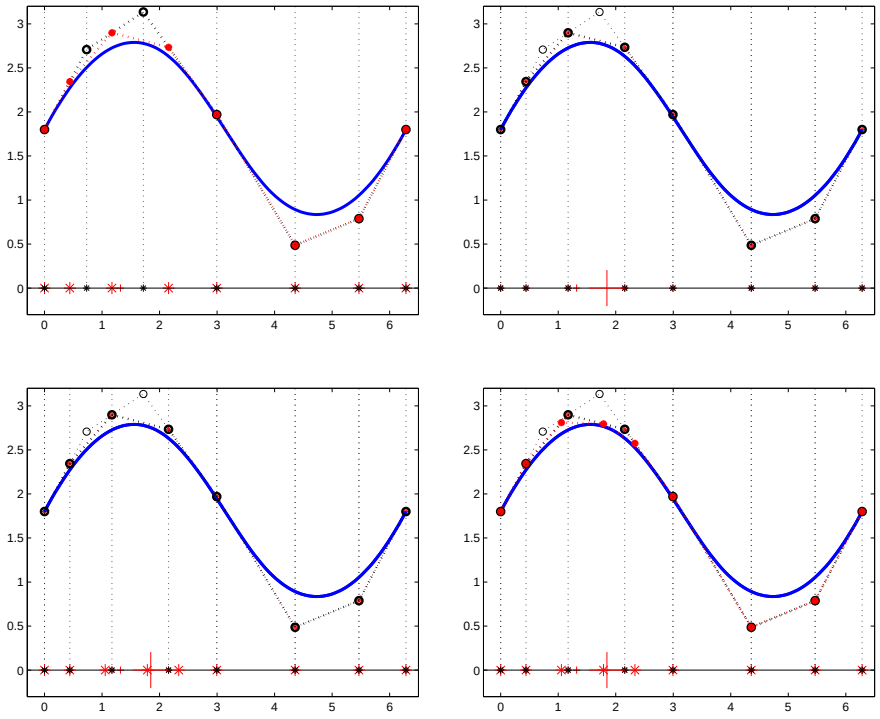

Fig. 17 Iterated knot insertion for cubic B-splines.

We may conclude that the number of sign changes in $\sum_j c_j B^{(p)}_{j,\Xi}(t)$ is bounded above by the number of sign changes in the sequence $\{...c_j...\}$. Thus, the B-spline basis provides a variation diminishing representation (see Corollary 1 and Proposition 1). Actually, by knot insertion the following fundamental result can be proved.

Theorem 7 (Karlin). *The B-spline basis is NTP.*

And (see Theorem 5)

Theorem 8. *The B-spline basis is the ONTP for piecewise polynomials.*

Remark 7. All the mentioned properties can be obtained by means of blossoming [30, 38].

Remark 8. Let us consider a knot interval $[\xi_r, \xi_{r+1}]$. A (possible) repeated insertion in the knot sequence of ξ_r and ξ_{r+1} so that each of them has multiplicity[2] $p+1$ (see example 6), the elements of the corresponding B-spline sequence not vanishing in the interval are the Bernstein polynomials. Therefore, the (repeated) knot insertion

[2] multiplicity p is actually sufficient for Bézier extraction

provides the conversion from the B-spline form to the Bézier-Bernstein one (**Bézier extraction**).

2.5 Degree elevation

We know that $\mathbb{P}_p \subset \mathbb{P}_{p+1}$, and taking into account (29), we consider the sequences of knots

$$\Xi := \{\ldots < \xi_r = \ldots = \xi_{r+\rho_r-1} < \ldots\} \subset \{\ldots < \xi_r = \ldots = \xi_{r+\rho_r} < \ldots\} =: \bar{\Xi}.$$

Therefore, $\mathbb{S}_{p,\Xi} \subset \mathbb{S}_{p+1,\bar{\Xi}}$.

Theorem 9.

$$B^{(p)}_{i,[\xi_i,\ldots,\xi_{i+p+1}]} = \frac{1}{p+1} \sum_{r=i}^{i+p+1} B^{(p+1)}_{r,[\xi_i,\ldots,\xi_r,\xi_r,\ldots,\xi_{i+p+1}]}$$

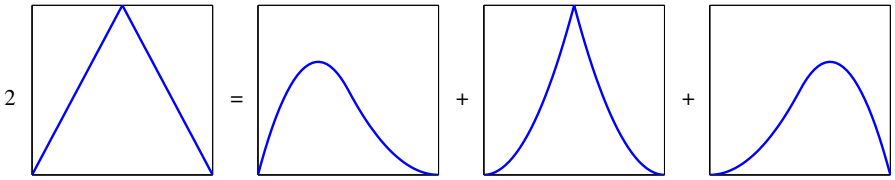

Fig. 18 Degree raising for a linear B-spline.

Remark 9. Repeated degree elevation leads to a sequence of control polygons that converges to the spline. Degree elevation/degree raising in CAGD corresponds to p-refinement in IgA.

2.6 Derivatives

$$\frac{\mathrm{d}}{\mathrm{d}t} B^{(p)}_{i,\Xi}(t) = p\left[\frac{1}{\xi_{i+p}-\xi_i} B^{(p-1)}_{i,\Xi}(t) - \frac{1}{\xi_{i+p+1}-\xi_{i+1}} B^{(p-1)}_{i+1,\Xi}(t)\right],$$

$$\frac{\mathrm{d}}{\mathrm{d}t} \sum_i c_i B^{(p)}_{i,\Xi}(t) = \sum_i p \frac{c_i - c_{i-1}}{\xi_{i+p}-\xi_i} B^{(p-1)}_{i,\Xi}(t).$$

In addition, the following integral recurrence relation holds

$$B^{(p)}_{i,\Xi}(t) = \delta^{(p-1)}_{i,\Xi} \int_{-\infty}^{t} B^{(p-1)}_{i,\Xi}(s)\mathrm{d}s - \delta^{(p-1)}_{i+1,\Xi} \int_{-\infty}^{t} B^{(p-1)}_{i+1,\Xi}(s)\mathrm{d}s, \tag{33}$$

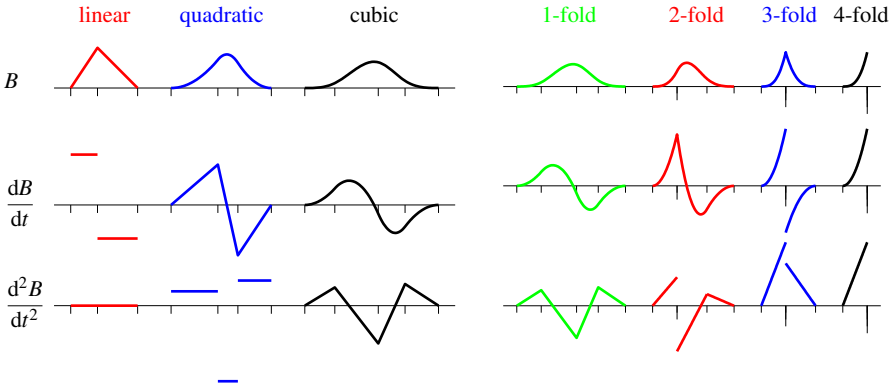

Fig. 19 Some B-splines and their derivatives.

$$\delta_{i,\Xi}^{(p)} := \frac{1}{\int_{-\infty}^{+\infty} B_{i,\Xi}^{(p)}(s)\mathrm{d}s}.$$

Remark 10. Using the knot sequence proposed in Example 6, the recurrence relation (33) reduces to (11). To recover the polynomials $B_i^{(p-1)}$, only a multiplicity of p is required, while for the polynomials $B_i^{(p)}$ a multiplicity of $p+1$ is needed. Therefore, there is a shift in indices comparing (11) and (33). The same shift of indices can be noted comparing (15) and (23).

2.7 NURBS: Non-Uniform Rational B-splineS

Definition 5. Given a set of B-splines and weights,

$$\{B_{i,\Xi}^{(p)}(t),\ i=1,\dots,\ n\},$$

$$W := \{w_i > 0,\ i=1,\dots,\ n\},$$

NURBS basis functions are defined by

$$R_{i,\Xi,W}^{(p)}(t) := \frac{w_i B_{i,\Xi}^{(p)}(t)}{\sum_{j=1}^{n} w_j B_{j,\Xi}^{(p)}(t)}.$$

NURBS curves are given by

$$\sum_i \mathbf{C}_i R_{i,\Xi,W}^{(p)}(t),\ \mathbf{C}_i \in \mathbb{R}^d.$$

NURBS immediately inherit from B-splines the following properties

- positivity
- partition of unity
- compact support
- smoothness
- TP

Moreover, a NURBS curve is projective transformation of a B-spline curve in $\mathbb{R}^{d+1}$

$$\left(\sum_i \mathbf{C}_i w_i B_{i,\Xi}^{(p)}(t),\ \sum_i w_i B_{i,\Xi}^{(p)}(t) \right). \tag{34}$$

Therefore, quadratic NURBS exactly represent (segments of) conic sections.

$$\frac{(1-t)^2 w_1 \mathbf{C}_1 + 2t(1-t) w_2 \mathbf{C}_2 + t^2 w_3 \mathbf{C}_3}{(1-t)^2 w_1 + 2t(1-t) w_2 + t^2 w_3}.$$

$\kappa := \frac{w_1 w_3}{w_2^2}$ is the **conic shape factor (CSF)**

$$\kappa = \begin{cases} < 1 & \text{hyperbola} \\ = 1 & \text{parabola} \\ > 1 & \text{ellipse} \end{cases},$$

without loss of generality $w_1 = w_3 = 1$.

Tensor-product NURBS surfaces can be easily defined

$$\Xi := \{\xi_1 \le \xi_2 \le \ldots \le \xi_{n+p+1}\},\ \Upsilon := \{\upsilon_1 \le \upsilon_2 \le \ldots \le \upsilon_{m+q+1}\}$$

$$\mathcal{S}(t,s) := \sum_{i=1,j=1}^{n,m} \mathbf{C}_{i,j} R_{i,j,\Xi,\Upsilon}^{(p,q)}(t,s)$$

$$R_{i,j,\Xi,\Upsilon}^{(p,q)}(t,s) := \frac{w_{i,j} B_{i,\Xi}^{(p)}(t) B_{j,\Upsilon}^{(q)}(s)}{\sum_{k=1,l=1}^{n,m} w_{k,l} B_{k,\Xi}^{(p)}(t) B_{l,\Upsilon}^{(q)}(s)},\ \ w_{i,j} > 0.$$

3 Beyond polynomials

3.1 Extended Chebyshev spaces

B-splines are a basis for piecewise polynomials i.e. piecewise functions with segments belonging to the space $\mathbb{P}_p = \langle 1, t, \ldots, t^{p-2}, t^{p-1}, t^p \rangle$. It is natural to replace such a space with some more general ones.

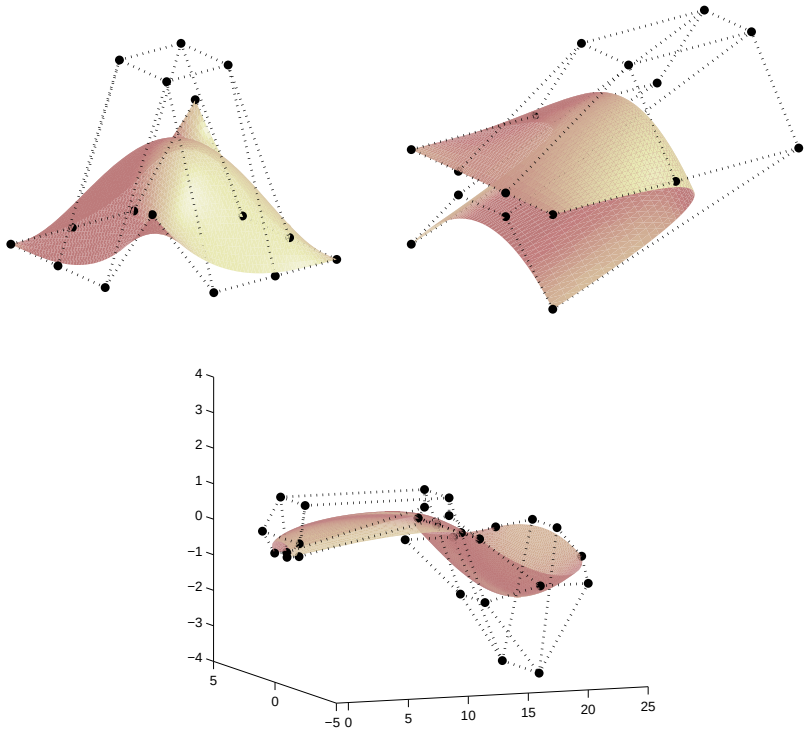

Fig. 20 Some tensor-product surfaces.

Definition 6. Let $\mathbb{E}$ be a space of dimension $p+1$ in I. $\mathbb{E}$ is an **Extended Chebyshev (EC) space** if any non-trivial element has at most p zeros in I, including their multiplicity.

Classical examples are all null spaces of linear differential operators of order $p+1$ with constant coefficients of which the characteristic polynomials have only real roots are EC spaces on $I=\mathbb{R}$. When the characteristic polynomial has at least one non-real root then the null space is an EC space only on a sufficiently small interval (at least on any interval of length $\frac{\pi}{a}$ where a denotes the greatest imaginary part of all non-real roots of the characteristic polynomial).

Theorem 10. *Let $\mathbb{E}$ be any $p+1$ dimensional space $\subset C^p(I)$, containing constants, such that the Wronskian of any basis of $\mathbb{E}$ does not vanish on the given interval.*[3] *Then the following properties are equivalent:*

- *$\mathbb{E}$ possesses an ONTP basis in any $(c,d)\subset I$;*
- *$\mathbb{E}' := \{f' : f \in \mathbb{E}\}$ is a p dimensional EC space on I.*

[3] This is always the case for an EC space.

Spaces of the form $\mathbb{E} = \mathbb{P}_p^{u,v}$

$$\mathbb{P}_p^{u,v} := \langle 1, t, \ldots, t^{p-2}, u(t), v(t) \rangle, \ p \geq 2, \ t \in I$$

are of special interest because they combine a "polynomial structure" with the ability of exactly representing salient profiles.

- The ONTP basis of $\mathbb{P}_p^{u,v}$,

$$\{B_{0,u,v}^{(p)}, \ldots, B_{p,u,v}^{(p)}\},$$

can be constructed imposing "end conditions" like Bernstein polynomials, see (8) and (9).

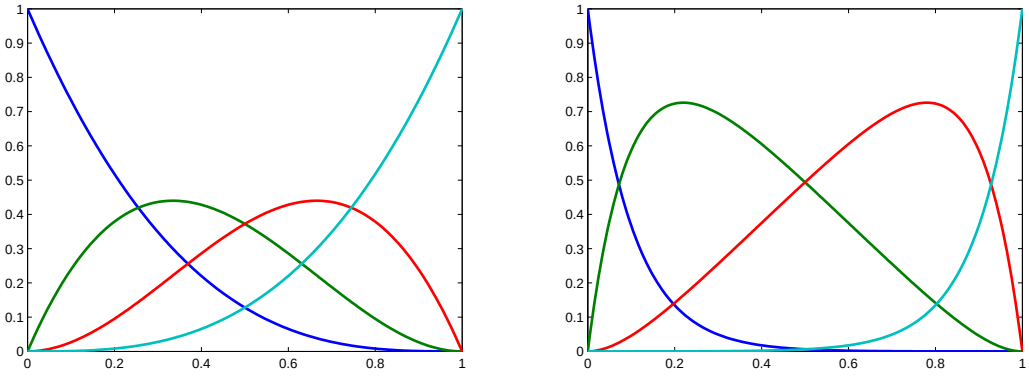

Fig. 21 The ONTP basis of $\mathbb{P}_3^{u,v}$. Left: $(u,v) = (\cos(\frac{\pi}{4}t), \sin(\frac{\pi}{4}t))$. Right: $(u,v) = (\cosh(10t), \sinh(10t))$.

- *Recurrence relation:* let us denote

$$U := \frac{\mathrm{d}^{p-1}}{\mathrm{d}t^{p-1}} u, \quad V := \frac{\mathrm{d}^{p-1}}{\mathrm{d}t^{p-1}} v,$$

and assume

$$\langle U, V \rangle \text{ is an EC space in } I. \tag{35}$$

With assumption (35), there exists a unique element in $\langle U, V \rangle$ which takes the values 0 and 1 (1 and 0) at the two ends of the interval I. Moreover, such an element has no other zeros in the interval, so it is positive in I. Therefore setting $I = [0, \ 1]$, without loss of generality we can assume

$$U(0) = 1, \ U(1) = 0, \quad V(0) = 0, \ V(1) = 1.$$

Then by setting

$$B_{0,u,v}^{(1)} := U, \quad B_{1,u,v}^{(1)} := V,$$

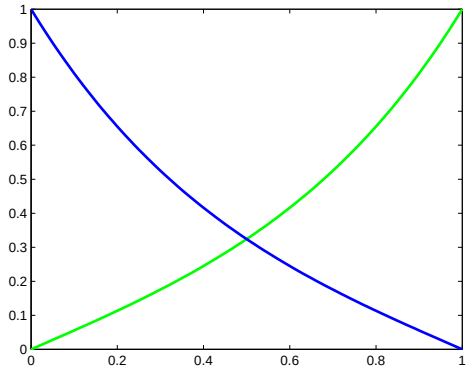

Fig. 22 $B^{(1)}_{0,u,v}, B^{(1)}_{1,u,v}$ with $(u,v) = (\cosh(3t), \sinh(3t))$.

we have (see (11))

$$B^{(p)}_{0,u,v}(t) = 1 - \delta^{(p-1)}_{0,u,v} \int_0^t B^{(p-1)}_{0,u,v}(s)\mathrm{d}s,$$
$$B^{(p)}_{i,u,v}(t) := \delta^{(p-1)}_{i-1,u,v} \int_0^t B^{(p-1)}_{i-1,u,v}(s)\mathrm{d}s - \delta^{(p-1)}_{i,u,v} \int_0^t B^{(p-1)}_{i,u,v}(s)\mathrm{d}s, \quad i = 1,\dots,p-1,$$
$$B^{(p)}_{p,u,v}(t) = \delta^{(p-1)}_{p-1} \int_0^t B^{(p-1)}_{p-1,u,v}(s)\mathrm{d}s,$$

with

$$\delta^{(p)}_{i,u,v} := \frac{1}{\int_0^1 B^{(p)}_{i,u,v}(s)\mathrm{d}s}.$$

- *Degree raising:* (see (16))

$$\mathbb{P}^{u,v}_p \subset \mathbb{P}^{u,v}_{p+1}$$
$$\sum_{i=0}^{p} \mathbf{P}_i B^{(p)}_{i,u,v}(t) = \sum_{i=0}^{p+1} \hat{\mathbf{P}}_i B^{(p+1)}_{i,u,v}(t)$$
$$\hat{\mathbf{P}}_0 := \mathbf{P}_0, \quad \hat{\mathbf{P}}_i := \theta_i \mathbf{P}_i + (1-\theta_i)\mathbf{P}_{i-1}, \quad \hat{\mathbf{P}}_{p+1} := \mathbf{P}_p,$$
$$\theta_i := \frac{\frac{\mathrm{d}^i}{\mathrm{d}t^i} B^{(p)}_{i,u,v}(0)}{\frac{\mathrm{d}^i}{\mathrm{d}t^i} B^{(p+1)}_{i,u,v}(0)}, \quad i = 1,\dots,p.$$

Example 7. The most popular choices for spaces $\mathbb{P}^{u,v}_p$ are

$$\mathbb{P}^{u,v}_p := \langle 1, \dots, t^{p-2}, \cos\omega t, \sin\omega t \rangle, \tag{36}$$

$$\mathbb{P}^{u,v}_p := \langle 1, \dots, t^{p-2}, \cosh\omega t, \sinh\omega t \rangle. \tag{37}$$

In such a case, assuming $I = [a,b]$, (35) reads

- $(u,v) = (\cos \omega t, \sin \omega t), \;\; 0 < \omega(b-a) < \pi,$
- $(u,v) = (\cosh \omega t, \sinh \omega t), \;\; 0 < \omega.$

3.2 Generalized B-splines

Let us consider spaces of functions belonging (piecewise) to $\mathbb{P}_p^{u_i,v_i}$. It is possible to construct a basis with the same properties as B-splines, the so-called generalized B-splines (GB-splines).
Let the knots $\Xi := \{\xi_1 \le \xi_2 \le \ldots \le \xi_{n+p+1}\}$ be given. Although more general constructions can be obtained with less restrictive hypotheses, a neat theory of GB-splines can be presented by assuming $u_i, v_i \in C^{p-1}[\xi_i, \xi_{i+1}]$ and

$$\langle U_i(t), V_i(t) \rangle, \;\; t \in [\xi_i, \xi_{i+1}], \;\; \text{is an EC space in } I, \tag{38}$$

where

$$U_i := \frac{\mathrm{d}^{p-1}}{\mathrm{d}t^{p-1}} u_i, \quad V_i := \frac{\mathrm{d}^{p-1}}{\mathrm{d}t^{p-1}} v_i.$$

Thus, as in the previous subsection, without loss of generality we can assume

$$U_i(\xi_i) = 1, \; U_i(\xi_{i+1}) = 0, \quad V_i(\xi_i) = 0, \; V_i(\xi_{i+1}) = 1.$$

According to [24], see also [29, 41] and the references therein, generalized B-splines $\widehat{B}_{i,\Xi}^{(p)}$ can be defined by the following recurrence relations completely similar to the classical polynomial case, see (33),

$$\widehat{B}_{i,\Xi}^{(1)}(t) := \begin{cases} V_i(t), & \text{if } t \in [\xi_i, \xi_{i+1}), \\ U_{i+1}(t), & \text{if } t \in [\xi_{i+1}, \xi_{i+2}), \\ 0, & \text{elsewhere}, \end{cases} \tag{39}$$

$$\widehat{B}_{i,\Xi}^{(p)}(t) := \widehat{\delta}_{i,\Xi}^{(p-1)} \int_{-\infty}^{t} \widehat{B}_{i,\Xi}^{(p-1)}(s)\mathrm{d}s - \widehat{\delta}_{i+1,\Xi}^{(p-1)} \int_{-\infty}^{t} \widehat{B}_{i+1,\Xi}^{(p-1)}(s)\mathrm{d}s \tag{40}$$

$$\widehat{\delta}_{i,\Xi}^{(p)} := \frac{1}{\int_{-\infty}^{+\infty} \widehat{B}_{i,\Xi}^{(p)}(s)\mathrm{d}s}$$

Example 8. GB-splines of salient interest are those with section spaces (36) and (37). We will refer to them as trigonometric GB-splines and exponential GB-splines, respectively.

Properties

- positivity
- partition of unity

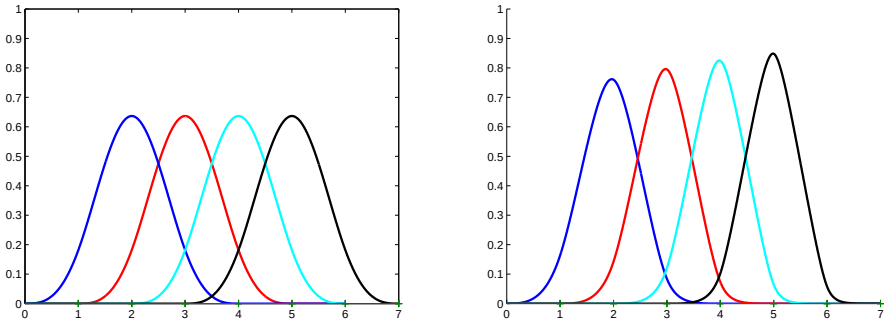

Fig. 23 Generalized cubic B-splines. Left: $(u_i, v_i) = (\cos(\frac{\pi}{2}t), \sin(\frac{\pi}{2}t))$. Right: $(u_i, v_i) = (\cosh(it), \sinh(it))$.

- compact support
- smoothness
- derivatives formulas
- local linear independence
- TP
- shape properties
- trigonometric and exponential parts can be mixed
- trigonometric and exponential GB-splines approach B-splines as the parameters approach 0.

Remark 11. GB-splines with sections in EC spaces possess all fundamental properties for design as B-splines, see [31]. In particular, corner cutting algorithms can be used for evaluation. Evaluation algorithms specially tuned for trigonometric and exponential GB-splines have been proposed by several authors, see for example [2, 27] and references therein. Stable evaluation can also be obtained by means of non-stationary subdivision [15].

4 Beyond tensor-product

4.1 Bézier-Bernstein representations on triangles

Let $T := \langle \mathbf{V}_1, \mathbf{V}_2, \mathbf{V}_3 \rangle$ be a nondegenerate triangle in $\mathbb{R}^2$ with $\mathbf{V}_i := (V_{i,x}, V_{i,y})$.

Definition 7. Any point $\mathbf{X} \in \mathbb{R}^2$ can be uniquely expressed in terms of its **barycentric coordinates** (τ_1, τ_2, τ_3) with respect to the triangle T, such that

$$\mathbf{X} = \tau_1 \mathbf{V}_1 + \tau_2 \mathbf{V}_2 + \tau_3 \mathbf{V}_3, \tag{41}$$

and

$$1 = \tau_1 + \tau_2 + \tau_3. \tag{42}$$

If the point $\mathbf{X}$ lies inside T, then its barycentric coordinates are all positive. The barycentric coordinates of the three vertices $\mathbf{V}_1$, $\mathbf{V}_2$ and $\mathbf{V}_3$ are $(1,0,0)$, $(0,1,0)$ and $(0,0,1)$, respectively.
The barycentric coordinates of the point $\mathbf{X}$ with respect to T have a clear geometric interpretation. For instance, τ_1 is the ratio between the signed area of the subtriangle $T_1 := \langle \mathbf{X}, \mathbf{V}_2, \mathbf{V}_3 \rangle$ and the signed area of the triangle T. A similar relation holds for τ_2 and τ_3, using the signed areas of the subtriangles $T_2 := \langle \mathbf{X}, \mathbf{V}_3, \mathbf{V}_1 \rangle$ and $T_3 := \langle \mathbf{X}, \mathbf{V}_1, \mathbf{V}_2 \rangle$, see Figure 24.

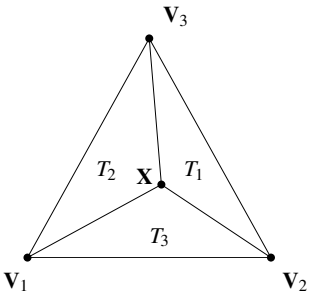

Fig. 24 Geometric interpretation of barycentric coordinates.

Definition 8. Given two points $\mathbf{X}_1$ and $\mathbf{X}_2$ in $\mathbb{R}^2$, the **barycentric directional coordinates** $(\delta_1, \delta_2, \delta_3)$ of the vector $\mathbf{X}_2 - \mathbf{X}_1$ with respect to T are defined as the difference of the barycentric coordinates of both points.

Example 9. The barycentric directional coordinates of the unit vectors $\mathbf{x}$ and $\mathbf{y}$ in the x- and y-direction, respectively, are given by

$$\begin{aligned}(\delta_1^x, \delta_2^x, \delta_3^x) &:= (V_{2,y} - V_{3,y}, V_{3,y} - V_{1,y}, V_{1,y} - V_{2,y})/E,\\ (\delta_1^y, \delta_2^y, \delta_3^y) &:= (V_{3,x} - V_{2,x}, V_{1,x} - V_{3,x}, V_{2,x} - V_{1,x})/E,\end{aligned}$$

with

$$E := \begin{vmatrix} V_{1,x} & V_{1,y} & 1 \\ V_{2,x} & V_{2,y} & 1 \\ V_{3,x} & V_{3,y} & 1 \end{vmatrix}. \tag{43}$$

Triangular Bernstein polynomials[4] of degree p are defined as follows

$$B_{i,j,k}^{(p)}(\mathbf{X}) := \frac{p!}{i!\,j!k!} {\tau_1}^i {\tau_2}^j {\tau_3}^k, \qquad \forall\, i+j+k = p, \tag{44}$$

[4] Along each edge of the triangle T, the triangular Bernstein polynomials reduce to the univariate Bernstein polynomials (1).

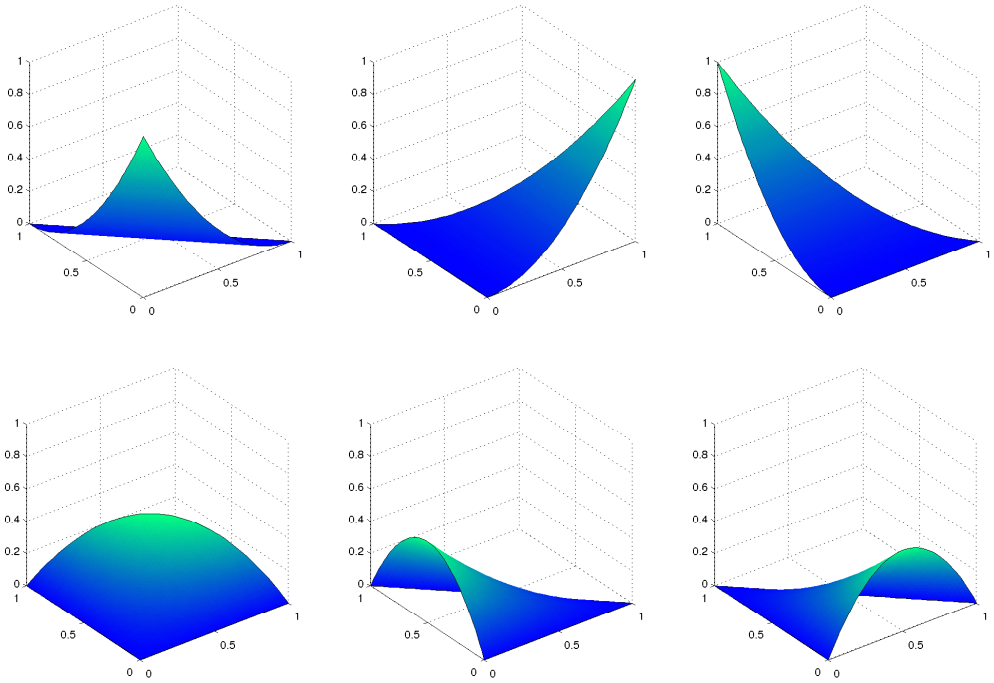

Fig. 25 Quadratic triangular Bernstein polynomials.

with (τ_1, τ_2, τ_3) the barycentric coordinates of $\mathbf{X}$. The Bernstein polynomials form a basis for the bivariate space of algebraic polynomials[5], i.e., any $q(\mathbf{X}) \in \mathbb{P}_p$ has a unique representation

$$q(\mathbf{X}) = \sum_{i+j+k=p} q_{i,j,k} B^{(p)}_{i,j,k}(\mathbf{X}). \tag{45}$$

We refer to $q_{i,j,k}$ as the **Bézier ordinates** of $q(\mathbf{X})$. Note that the dimension of $\mathbb{P}_p$ is equal to $\binom{p+2}{2}$. The triangular Bernstein polynomials possess properties similar to the univariate case.

- *Positivity:*

$$B^{(p)}_{i,j,k}(\mathbf{X}) \geq 0, \quad \mathbf{X} \in T. \tag{46}$$

- *Partition of unity:*

$$\sum_{i+j+k=p} B^{(p)}_{i,j,k}(\mathbf{X}) = (\tau_1 + \tau_2 + \tau_3)^p = 1, \quad \forall\, \mathbf{X} \in \mathbb{R}^2. \tag{47}$$

[5] In both the univariate and bivariate case we use the same symbol for the space of algebraic polynomials, $\mathbb{P}_p$, but the meaning will be clear from the context.

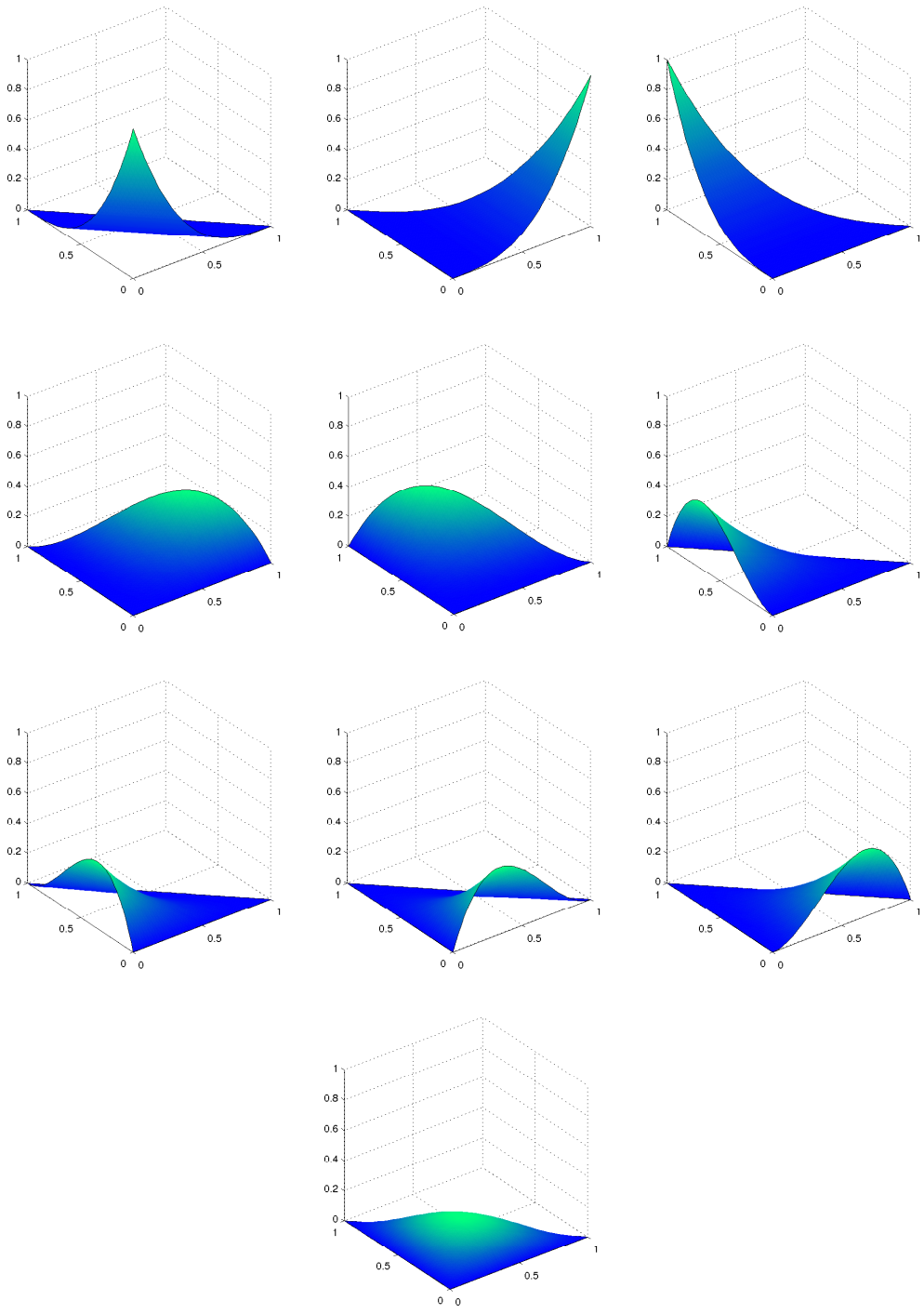

Fig. 26 Cubic triangular Bernstein polynomials.

- *Recurrence relation:*

$$B^{(p)}_{i,j,k}(\mathbf{X}) = \tau_1 B^{(p-1)}_{i-1,j,k}(\mathbf{X}) + \tau_2 B^{(p-1)}_{i,j-1,k}(\mathbf{X}) + \tau_3 B^{(p-1)}_{i,j,k-1}(\mathbf{X}), \tag{48}$$

  with $B^{(l)}_{i,j,k} = 0$ if $i < 0$ or $j < 0$ or $k < 0$.
- *Degree raising/degree elevation:*

$$\begin{aligned} B^{(p)}_{i,j,k}(\mathbf{X}) &= (\tau_1 + \tau_2 + \tau_3) B^{(p)}_{i,j,k}(\mathbf{X}) \\ &= \frac{i+1}{p+1} B^{(p+1)}_{i+1,j,k}(\mathbf{X}) + \frac{j+1}{p+1} B^{(p+1)}_{i,j+1,k}(\mathbf{X}) + \frac{k+1}{p+1} B^{(p+1)}_{i,j,k+1}(\mathbf{X}). \end{aligned} \tag{49}$$

- *Integration:*

$$\int_T B^{(p)}_{i,j,k}(\mathbf{X})\,\mathrm{d}\mathbf{X} = \frac{|E|}{2\binom{p+2}{2}}, \tag{50}$$

$$\int_T B^{(p)}_{i_1,j_1,k_1}(\mathbf{X})\, B^{(p)}_{i_2,j_2,k_2}(\mathbf{X})\,\mathrm{d}\mathbf{X} = \frac{\binom{i_1+i_2}{i_1}\binom{j_1+j_2}{j_1}\binom{k_1+k_2}{k_1}|E|}{2\binom{2p}{p}\binom{2p+2}{2}}, \tag{51}$$

  where E is defined in (43). Note that $|E|/2$ is the area of the triangle T.
- *Directional derivatives:* Let $\mathbf{u}$ be a unit vector in $\mathbb{R}^2$ and let $(\delta_1, \delta_2, \delta_3)$ be its barycentric directional coordinates with respect to the triangle T.
  - first derivative:

$$D_{\mathbf{u}} B^{(p)}_{i,j,k}(\mathbf{X}) = p[\delta_1 B^{(p-1)}_{i-1,j,k}(\mathbf{X}) + \delta_2 B^{(p-1)}_{i,j-1,k}(\mathbf{X}) + \delta_3 B^{(p-1)}_{i,j,k-1}(\mathbf{X})]; \tag{52}$$

  - end derivatives:

$$D^r_{\mathbf{u}} B^{(p)}_{i,j,k}(\mathbf{V}_1) = 0, \quad r = 0, \ldots, p-i-1; \tag{53}$$

$$D^r_{\mathbf{u}} B^{(p)}_{i,j,k}(\mathbf{V}_2) = 0, \quad r = 0, \ldots, p-j-1; \tag{54}$$

$$D^r_{\mathbf{u}} B^{(p)}_{i,j,k}(\mathbf{V}_3) = 0, \quad r = 0, \ldots, p-k-1; \tag{55}$$

  - unimodal behavior:

$$D_{\mathbf{u}} B^{(p)}_{i,j,k}(\boldsymbol{\xi}^*_{i,j,k}) = 0, \quad \text{iff } i \geq 1,\ j \geq 1,\ k \geq 1, \tag{56}$$

    and

$$\boldsymbol{\xi}^*_{i,j,k} := \frac{i\mathbf{V}_1 + j\mathbf{V}_2 + k\mathbf{V}3}{p}. \tag{57}$$

Example 10. Considering $q(\mathbf{X}) = \mathbf{X}$, we have

$$\mathbf{X} = \sum_{i+j+k=p} \boldsymbol{\xi}^*_{i,j,k} B^{(p)}_{i,j,k}(\mathbf{X}). \tag{58}$$

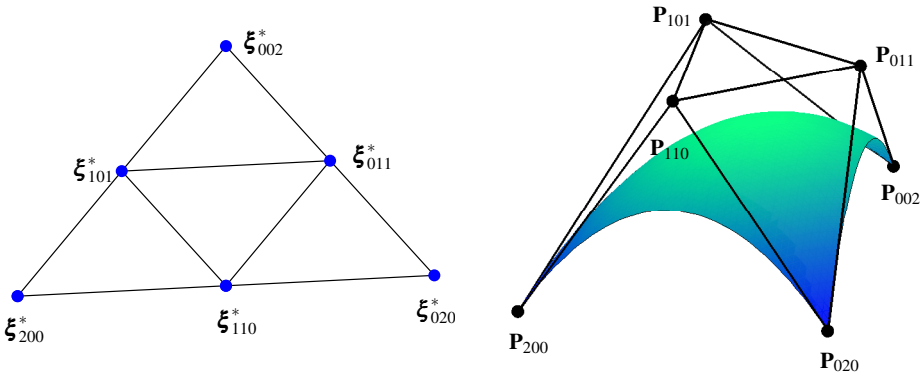

Fig. 27 Left: quadratic domain points. Right: control net of a quadratic polynomial.

The points $\boldsymbol{\xi}^*_{i,j,k}$, defined in (57), are called **Greville abscissas** or **domain points**. The set of all these points is denoted by $\mathcal{D}_{p,T}$. They are uniformly spaced over the triangle T, and they can be triangulated by connecting each pair of two domain points $\boldsymbol{\xi}^*_{i_1,j_1,k_1}$ and $\boldsymbol{\xi}^*_{i_2,j_2,k_2}$ provided that

$$|i_1 - i_2| + |j_1 - j_2| + |k_1 - k_2| = 2, \tag{59}$$

see Figure 27 (left) for the quadratic case.

The above properties lead again to a number of interesting geometric consequences. Let $\mathbf{P}_{i,j,k} \in \mathbb{R}^d$, $i+j+k=p$, be given. The parametric surface

$$\mathcal{S}(\mathbf{X}) := \sum_{i+j+k=p} \mathbf{P}_{i,j,k} B^{(p)}_{i,j,k}(\mathbf{X})$$

is called a **Bézier surface**, and the points $\mathbf{P}_{i,j,k}$ are its **control points**. The piecewise linear interpolant connecting these points as given by (59) is called the **control net** of $\mathcal{S}(\mathbf{X})$. The graph of any polynomial $q(\mathbf{X})$ in (45) can be seen as a Bézier surface

$$\begin{pmatrix} \mathbf{X} \\ q(\mathbf{X}) \end{pmatrix} = \sum_{i+j+k=p} \begin{pmatrix} \boldsymbol{\xi}^*_{i,j,k} \\ q_{i,j,k} \end{pmatrix} B^{(p)}_{i,j,k}(\mathbf{X}),$$

and the piecewise linear interpolant connecting $\begin{pmatrix} \boldsymbol{\xi}^*_{i,j,k} \\ q_{i,j,k} \end{pmatrix}$ is its control net. Figure 27 (right) illustrates the control net of a quadratic Bézier surface.

- The positivity and partition of unity imply the convex hull property: $\mathcal{S}(\mathbf{X}) \in \mathcal{H}(\mathbf{P}_{i,j,k},\ i+j+k=p)$.
- The recurrence relation (48) leads to a stable evalutation algorithm, a triangular variant of the de Casteljau algorithm:

$$\begin{aligned}\mathcal{S}(\mathbf{X}) &= \sum_{i+j+k=p} \mathbf{P}^{[p]}_{i,j,k} B^{(p)}_{i,j,k}(\mathbf{X}) \\ &= \sum_{i+j+k=p} \mathbf{P}^{[p]}_{i,j,k} [\tau_1 B^{(p-1)}_{i-1,j,k}(\mathbf{X}) + \tau_2 B^{(p-1)}_{i,j-1,k}(\mathbf{X}) + \tau_3 B^{(p-1)}_{i,j,k-1}(\mathbf{X})] \\ &= \sum_{i+j+k=p-1} \mathbf{P}^{[p-1]}_{i,j,k} B^{(p-1)}_{i,j,k}(\mathbf{X}) = \ldots = \mathbf{P}^{[0]}_{0,0,0},\end{aligned}$$

with (τ_1, τ_2, τ_3) the barycentric coordinates of $\mathbf{X}$, and

$$\mathbf{P}^{[l-1]}_{i,j,k} := \tau_1 \mathbf{P}^{[l]}_{i+1,j,k} + \tau_2 \mathbf{P}^{[l]}_{i,j+1,k} + \tau_3 \mathbf{P}^{[l]}_{i,j,k+1}, \quad i+j+k = l-1. \tag{60}$$

This algorithm provides a very efficient tool to evaluate a Bézier surface at a given parameter value $\mathbf{X} \in T$.

- By using (49), and by setting $\mathbf{P}_{i,j,k} = 0$ if $i < 0$ or $j < 0$ or $k < 0$, we obtain

$$\sum_{i+j+k=p} \mathbf{P}_{i,j,k} B^{(p)}_{i,j,k}(\mathbf{X}) = \sum_{i+j+k=p+1} \hat{\mathbf{P}}_{i,j,k} B^{(p+1)}_{i,j,k}(\mathbf{X}), \tag{61}$$

with

$$\hat{\mathbf{P}}_{i,j,k} := \frac{i}{p+1}\mathbf{P}_{i-1,j,k} + \frac{j}{p+1}\mathbf{P}_{i,j-1,k} + \frac{k}{p+1}\mathbf{P}_{i,j,k-1}.$$

- Let $\mathbf{u}$ be a unit vector in $\mathbb{R}^2$ and let $(\delta_1, \delta_2, \delta_3)$ be its barycentric directional coordinates with respect to the triangle T. Directional derivatives of Bézier surfaces are obtained by applying (52):

$$D_{\mathbf{u}}\mathcal{S}(\mathbf{X}) = p \sum_{i+j+k=p-1} [\delta_1 \mathbf{P}_{i+1,j,k} + \delta_2 \mathbf{P}_{i,j+1,k} + \delta_3 \mathbf{P}_{i,j,k+1}] B^{(p-1)}_{i,j,k}(\mathbf{X}). \tag{62}$$

More generally, the r-th order directional derivative equals

$$D^r_{\mathbf{u}}\mathcal{S}(\mathbf{X}) = \frac{p!}{(p-r)!} \sum_{i+j+k=p-r} \Delta_r(\mathbf{P}_{i,j,k}) B^{(p-r)}_{i,j,k}(\mathbf{X}), \tag{63}$$

where $\Delta_r(\mathbf{P}_{i,j,k}) := \mathbf{P}^{[p-r]}_{i,j,k}$ are the quantities (60) obtained after r steps of the triangular de Casteljau algorithm applied to the control points of $\mathcal{S}(\mathbf{X})$ using the barycentric directional coordinates of $\mathbf{u}$.

- From (62) it follows that the derivative at the vertex $\mathbf{V}_1$ can be written as

$$D_{\mathbf{u}}\mathcal{S}(\mathbf{V}_1) = p[\delta_1 \mathbf{P}_{p,0,0} + \delta_2 \mathbf{P}_{p-1,1,0} + \delta_3 \mathbf{P}_{p-1,0,1}],$$

implying that the control net is tangent to the surface at the three corner points. More generally, $\binom{r+2}{2}$ control points are involved in the expression of $D^r_{\mathbf{u}}\mathcal{S}(\mathbf{V}_i)$.

- C^r continuity between two adjacent Bézier surfaces

$$\sum_{i+j+k=p} \mathbf{P}^L_{i,j,k} B^{(p)}_{i,j,k}(\mathbf{X}), \qquad \sum_{i+j+k=p} \mathbf{P}^R_{i,j,k} B^{(p)}_{i,j,k}(\mathbf{X}),$$

defined on the triangles $T_L := \langle \mathbf{V}_1, \mathbf{V}_2, \mathbf{V}_3 \rangle$ and $T_R := \langle \mathbf{V}_1, \mathbf{V}_2, \mathbf{V}_4 \rangle$ respectively, has a simple geometric interpretation thanks to the local behavior of the derivatives at the end points, see (62) and (63). In particular, C^0 continuity just requires that $\mathbf{P}^L_{i,j,0} = \mathbf{P}^R_{i,j,0}$ for all $i+j=p$, while C^1 continuity implies, in addition, that for each $i+j=p-1$ the pair of triangles

$$\langle \mathbf{P}^L_{i,j,1}, \mathbf{P}^L_{i+1,j,0}, \mathbf{P}^L_{i,j+1,0} \rangle, \quad \langle \mathbf{P}^R_{i,j,1}, \mathbf{P}^R_{i+1,j,0}, \mathbf{P}^R_{i,j+1,0} \rangle$$

are coplanar, see Figure 28.

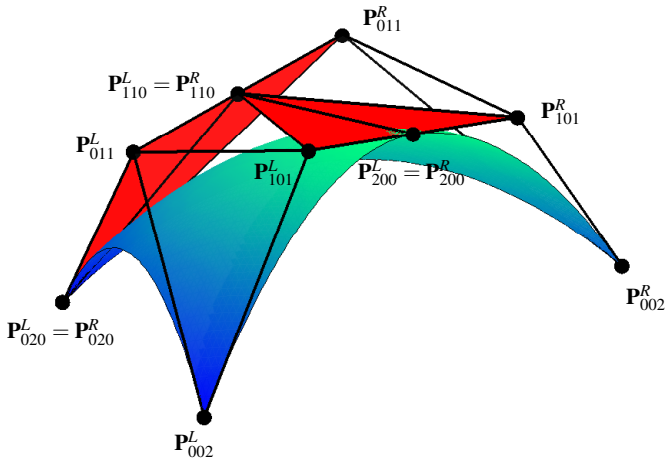

Fig. 28 C^1 joint between two quadratic Bézier surfaces.

4.2 Splines on triangulations

Definition 9. A **triangulation** $\mathcal{T} := \{T_i,\ i = 1,\dots,N_t\}$ of a polygonal set $\Omega \subseteq \mathbb{R}^2$ is a partition of Ω consisting of non-overlapping triangles. No triangle $T_i \in \mathcal{T}$ contains a vertex of any other triangle $T_j \in \mathcal{T}$ that is different from its own three vertices.

Definition 10. Given a triangulation $\mathcal{T}$ of Ω the **spline space** of degree p on $\mathcal{T}$ with C^r continuity is defined as

$$\mathbb{S}^r_{p,\mathcal{T}} := \left\{ s \in C^r(\Omega) : s_{|T_i} \in \mathbb{P}_p,\ T_i \in \mathcal{T} \right\}. \tag{64}$$

As we have seen, it is convenient to represent polynomials on triangles in their Bézier-Bernstein form. We can use this form for the characterization of splines defined on triangulations. The **set of domain points** of degree p associated to the

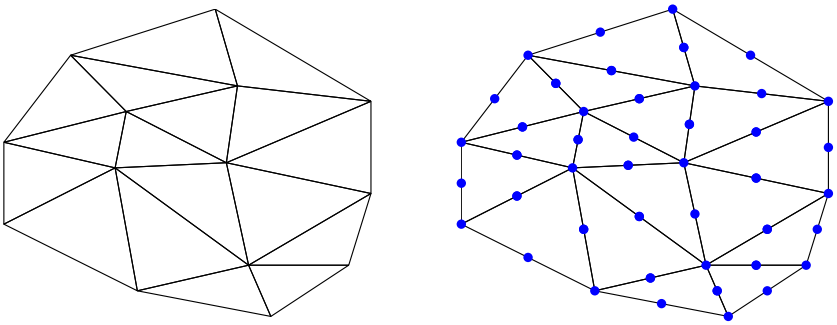

Fig. 29 A triangulation $\mathcal{T}$, and its set of quadratic domain points $\mathcal{D}_{2,\mathcal{T}}$.

triangulation $\mathcal{T}$ is denoted by

$$\mathcal{D}_{p,\mathcal{T}} := \bigcup_{T_i \in \mathcal{T}} \mathcal{D}_{p,T_i},$$

i.e., the union of all domain points (57) on each triangle $T_i \in \mathcal{T}$. Figure 29 (right) illustrates the set of quadratic domain points for a given triangulation.

Let N_t, N_v and N_e be the number of triangles, vertices and edges in $\mathcal{T}$. The dimension of $\mathbb{S}^0_{p,\mathcal{T}}$ is equal to the number of domain points in $\mathcal{D}_{p,\mathcal{T}}$, i.e.,

$$N_v + (p-1)N_e + \binom{p-1}{2} N_t.$$

For any spline $s \in \mathbb{S}^0_{p,\mathcal{T}}$ there exists a unique set of coefficients $\left\{c_{\boldsymbol{\xi}},\ \boldsymbol{\xi} \in \mathcal{D}_{p,\mathcal{T}}\right\}$ such that for each $T_i \in \mathcal{T}$

$$s_{|T_i} = \sum_{\boldsymbol{\xi} \in \mathcal{D}_{p,T_i}} c_{\boldsymbol{\xi}} B^{(p)}_{\boldsymbol{\xi},T_i|T_i},$$

where $B^{(p)}_{\boldsymbol{\xi},T_i}$ is the Bernstein polynomial (44) of degree p associated to the triangle T_i and to the triple of indices defining $\boldsymbol{\xi}$ with respect to T_i, see (57). The set of functions $\left\{P^{(p)}_{\boldsymbol{\xi},\mathcal{T}}(\mathbf{X}),\ \boldsymbol{\xi} \in \mathcal{D}_{p,\mathcal{T}}\right\}$ defined by

$$P^{(p)}_{\boldsymbol{\xi},\mathcal{T}}(\mathbf{X}) := \begin{cases} B^{(p)}_{\boldsymbol{\xi},T_i}(\mathbf{X}), & \text{if } \boldsymbol{\xi} \in \mathcal{D}_{p,T_i},\ \mathbf{X} \in T_i,\ T_i \in \mathcal{T}, \\ 0, & \text{elsewhere}, \end{cases} \tag{65}$$

forms a basis for $\mathbb{S}^0_{p,\mathcal{T}}$, with the properties:

- positivity
- partition of unity
- compact support

Remark 12. A common basis for $\mathbb{S}^0_{p,\mathcal{T}}$ in the finite element literature is a Lagrange-type basis $\left\{L^{(p)}_{\boldsymbol{\xi},\mathcal{T}}(\mathbf{X}),\ \boldsymbol{\xi}\in\mathcal{D}_{p,\mathcal{T}}\right\}$. These basis functions are defined as the unique interpolant of the problem

$$L^{(p)}_{\boldsymbol{\xi},\mathcal{T}}(\boldsymbol{\eta})=\delta_{\boldsymbol{\xi},\boldsymbol{\eta}},\quad \text{for all } \boldsymbol{\eta}\in\mathcal{D}_{p,\mathcal{T}},$$

where $\delta_{\boldsymbol{\xi},\boldsymbol{\eta}}$ denotes the Kronecker symbol. These basis functions are not positive.

In IgA spline spaces of higher smoothness are of interest. Smoothness conditions on a spline $s\in\mathbb{S}^0_{p,\mathcal{T}}$ are just linear conditions on the vector $\mathbf{c}$ of coefficients of s, see (62)–(63). Thus, given a set of smoothness conditions $\mathfrak{S}$, there is a matrix $A^{\mathfrak{S}}$ so that

$$\mathbb{S}^{\mathfrak{S}}_{p,\mathcal{T}}:=\left\{s\in\mathbb{S}^0_{p,\mathcal{T}}:A^{\mathfrak{S}}\mathbf{c}=0\right\}. \tag{66}$$

The matrix $A^{\mathfrak{S}}$ is of size $m\times n$, with m the number of smoothness conditions in $\mathfrak{S}$ and n the dimension of $\mathbb{S}^0_{p,\mathcal{T}}$.

Theorem 11. *Let $\mathbb{S}^{\mathfrak{S}}_{p,\mathcal{T}}$ be a smooth spline space as defined in (66), then the dimension of $\mathbb{S}^{\mathfrak{S}}_{p,\mathcal{T}}$ is equal to $n-k$, with k the rank of the matrix $A^{\mathfrak{S}}$.*

Remark 13. The computation of the dimension of smooth spline spaces defined on triangulations is a difficult task. There exist very sharp lower bounds and good upper bounds on the dimension of spline spaces for any combination of degree and smoothness, but there are still spaces for which no exact dimension formula is known, for instance the space $\mathbb{S}^1_{3,\mathcal{T}}$. We refer to [25] for a detailed discussion of the problem and an overview of smooth spline spaces on triangulations.

Remark 14. The dimension problem is linked to the construction of a so-called **minimal determining set** of domain points [25]. This is a subset $\mathcal{M}\subseteq\mathcal{D}_{p,\mathcal{T}}$ of minimal cardinality such that if $s\in\mathbb{S}^r_{p,\mathcal{T}}$ and $c_{\boldsymbol{\xi}}=0$ for all $\boldsymbol{\xi}\in\mathcal{M}$, then $s\equiv 0$. The cardinality of $\mathcal{M}$ is equal to the dimension of $\mathbb{S}^r_{p,\mathcal{T}}$.

Remark 15. The dimension of such spline spaces should be preferably expressed only in terms of geometrically interesting characteristics of the triangulation (like the number of vertices, edges, and triangles). Imposing additional local super-smoothness and/or considering triangulations with a particular macro-structure may simplify the dimension formula, and also the construction of a suitable basis (an example is elaborated in the next subsection).

Remark 16. Instead of defining first a particular spline space on a triangulation and then finding a suitable basis, one can also proceed the other way around: choose first a set of individual B-like spline functions, and then define the spline space as the span of these functions. For example,

- box splines, see [5];
- simplex splines, see [4, 32, 33].

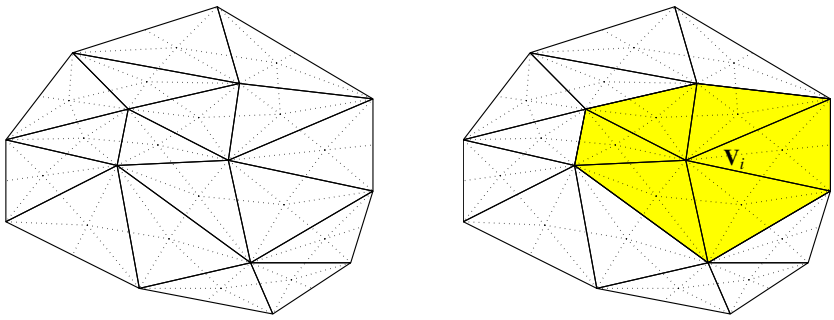

Fig. 30 Left: a PS refinement $\mathcal{T}^*$ of the triangulation $\mathcal{T}$ in Figure 29. Right: the molecule Ω_i of a vertex $\mathbf{V}_i$ of $\mathcal{T}$.

4.3 Powell-Sabin B-splines

Definition 11. A **Powell-Sabin refinement** $\mathcal{T}^*$ of $\mathcal{T}$ is the refined triangulation obtained by subdividing each triangle of $\mathcal{T}$ into six smaller triangles as follows (see also Figure 30).

1. Select a point $\mathbf{Z}_i$ inside each triangle T_i of $\mathcal{T}$ so that, if two triangles T_i and T_j have a common edge, then the line joining $\mathbf{Z}_i$ and $\mathbf{Z}_j$ intersects the common edge at a point $\mathbf{R}_{i,j}$.[6]
2. Join each point $\mathbf{Z}_i$ to the vertices of T_i.
3. For each edge of the triangle T_i
   a. which is common to a triangle T_j: join $\mathbf{Z}_i$ to $\mathbf{R}_{i,j}$;
   b. which belongs to the boundary $\partial\Omega$: join $\mathbf{Z}_i$ to an arbitrary point $\mathbf{R}^b_{i,j}$ on that edge.[7]

Definition 12 ([35]). Given a triangulation $\mathcal{T}$ of Ω and a PS refinement $\mathcal{T}^*$, the space of piecewise quadratic polynomials on $\mathcal{T}^*$ with global C^1 continuity is called the **Powell-Sabin spline space**:

$$\mathbb{S}^1_{2,\mathcal{T}^*} := \left\{ s \in C^1(\Omega) : s_{|T_i^*} \in \mathbb{P}_2,\ T_i^* \in \mathcal{T}^* \right\}. \tag{67}$$

Let $\{\mathbf{V}_k,\ k = 1,\ldots,N_v\}$ be the set of vertices of $\mathcal{T}$. It is known that the dimension of $\mathbb{S}^1_{2,\mathcal{T}^*}$ is equal to $3N_v$.

[6] Such a choice is always possible: $\mathbf{Z}_i$ can be selected as the center of the inscribed circle. Usually, the barycenter of T_i is also a valid choice (but not always).

[7] For boundary edges the subscript j refers to the edge.

Theorem 12. *Given a set of triplets $(f_k, f_{x,k}, f_{y,k})$ at the vertices $\mathbf{V}_k$, $k = 1, \ldots, N_v$, there exists a unique Powell-Sabin spline $s \in \mathbb{S}^1_{2,\mathcal{T}^*}$ that satisfies*

$$s(\mathbf{V}_k) = f_k, \quad D_{\mathbf{x}} s(\mathbf{V}_k) = f_{x,k}, \quad D_{\mathbf{y}} s(\mathbf{V}_k) = f_{y,k}. \tag{68}$$

This interpolation problem turns out to be particularly useful for constructing a local basis for $\mathbb{S}^1_{2,\mathcal{T}^*}$.

Dierckx [13] presented a geometric method to construct a normalized basis $\{B_{i,j,\mathcal{T}^*}(\mathbf{X}),\ j = 1,2,3,\ i = 1, \ldots, N_v\}$ for the spline space $\mathbb{S}^1_{2,\mathcal{T}^*}$, such that

$$s(\mathbf{X}) = \sum_{i=1}^{N_v} \sum_{j=1}^{3} c_{i,j} B_{i,j,\mathcal{T}^*}(\mathbf{X}), \tag{69}$$

for all $s \in \mathbb{S}^1_{2,\mathcal{T}^*}$, and

- *Positivity:* $B_{i,j,\mathcal{T}^*} \geq 0$.
- *Partition of unity:* $\sum_{i=1}^{N_v} \sum_{j=1}^{3} B_{i,j,\mathcal{T}^*} = 1$.
- *Compact support:* $B_{i,j,\mathcal{T}^*}$ is zero outside the molecule Ω_i of the vertex $\mathbf{V}_i$, which is the subset of Ω consisting of the points belonging to the union of all triangles of $\mathcal{T}$ containing the vertex $\mathbf{V}_i$, see Figure 30.

The functions $B_{i,j,\mathcal{T}^*}$ will be referred to as **Powell-Sabin B-splines**. To locally construct these PS B-splines $B_{i,j,\mathcal{T}^*}$, $j = 1,2,3$, with support in Ω_i, it suffices to specify their values and gradients at any vertex of $\mathcal{T}$. Due to the structure of the support Ω_i, we have

$$B_{i,j,\mathcal{T}^*}(\mathbf{V}_k) = 0, \quad D_{\mathbf{x}} B_{i,j,\mathcal{T}^*}(\mathbf{V}_k) = 0, \quad D_{\mathbf{y}} B_{i,j,\mathcal{T}^*}(\mathbf{V}_k) = 0, \tag{70}$$

for any vertex $\mathbf{V}_k \neq \mathbf{V}_i$. We set

$$B_{i,j,\mathcal{T}^*}(\mathbf{V}_i) =: \alpha_{i,j}, \quad D_{\mathbf{x}} B_{i,j,\mathcal{T}^*}(\mathbf{V}_i) =: \beta_{i,j}, \quad D_{\mathbf{y}} B_{i,j,\mathcal{T}^*}(\mathbf{V}_i) =: \gamma_{i,j}. \tag{71}$$

For each vertex $\mathbf{V}_i$, let us consider three points

$$\{\mathbf{Q}_{i,j} := (Q_{i,j,x}, Q_{i,j,y}),\ j = 1,2,3\}$$

such that, for $i = 1, \ldots, N_v$,

$$\begin{pmatrix} \alpha_{i,1} & \alpha_{i,2} & \alpha_{i,3} \\ \beta_{i,1} & \beta_{i,2} & \beta_{i,3} \\ \gamma_{i,1} & \gamma_{i,2} & \gamma_{i,3} \end{pmatrix} \begin{pmatrix} Q_{i,1,x} & Q_{i,1,y} & 1 \\ Q_{i,2,x} & Q_{i,2,y} & 1 \\ Q_{i,3,x} & Q_{i,3,y} & 1 \end{pmatrix} = \begin{pmatrix} V_{i,x} & V_{i,y} & 1 \\ 1 & 0 & 0 \\ 0 & 1 & 0 \end{pmatrix}. \tag{72}$$

It follows that

$$\mathbf{X} = \sum_{i=1}^{N_v} \sum_{j=1}^{3} \mathbf{Q}_{i,j} B_{i,j,\mathcal{T}^*}(\mathbf{X}), \tag{73}$$

so, the points $\mathbf{Q}_{i,j}$ are the Greville abscissas for the basis functions $B_{i,j,\mathcal{T}^*}$. The triangle $\mathfrak{T}_i := \langle \mathbf{Q}_{i,1}, \mathbf{Q}_{i,2}, \mathbf{Q}_{i,3} \rangle$ is referred to as **PS triangle** associated to the vertex $\mathbf{V}_i$.

From (72) it follows that for each vertex $\mathbf{V}_l$ the three functions $B_{i,j,\mathcal{T}^*}$, $j = 1,2,3$, are uniquely determined by the points $\{\mathbf{Q}_{i,j},\ j = 1,2,3\}$. Moreover,

- $(\alpha_{i,1}, \alpha_{i,2}, \alpha_{i,3})$ are the barycentric coordinates of the vertex $\mathbf{V}_i$ with respect to the triangle $\mathfrak{T}_i$;
- $(\beta_{i,1}, \beta_{i,2}, \beta_{i,3})$ are the barycentric directional coordinates of the x-direction with respect to $\mathfrak{T}_i$;
- $(\gamma_{i,1}, \gamma_{i,2}, \gamma_{i,3})$ are the barycentric directional coordinates of the y-direction with respect to $\mathfrak{T}_i$;
- at vertex $\mathbf{V}_i$, the basis function $B_{i,j,\mathcal{T}^*}$ has a directional derivative equal to zero in the direction of the edge of $\mathfrak{T}_i$ opposite to $\mathbf{Q}_{i,j}$.

Finally, for each vertex $\mathbf{V}_i$ we define its **PS points** as the vertex itself and the midpoints of all the edges of the PS refinement $\mathcal{T}^*$ containing $\mathbf{V}_i$, see Figure 31. Then we have the following result (see also Figures 31 and 32).

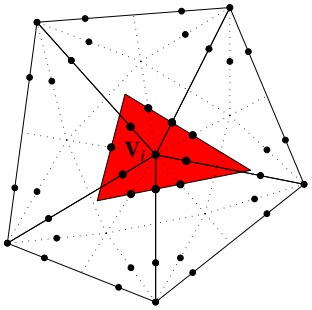

Fig. 31 Location of the PS points (black bullets), and a possible PS triangle for the vertex $\mathbf{V}_i$ (shaded), see Theorem 13.

Theorem 13 ([13]). *The functions $B_{i,j,\mathcal{T}^*}$, $j = 1,2,3$, are positive if and only if the PS triangle $\mathfrak{T}_i$ contains all the PS points associated to the vertex $\mathbf{V}_i$.*

Summarizing, the PS B-splines associated to each vertex $\mathbf{V}_i$ of $\mathcal{T}$ are uniquely associated to the triple of points $\mathbf{Q}_{i,j}$, $j = 1,2,3$, forming the PS triangle. Hence, PS triangles can be efficiently used to geometrically identify and describe the PS B-splines and their properties instead of $\alpha_{i,j}$, $\beta_{i,j}$, $\gamma_{i,j}$.

Combining (69) and (73) leads to the definition of **PS control points**:

$$\mathbf{C}_{i,j} = (\mathbf{Q}_{i,j}, c_{i,j}),$$

forming the **PS control triangles** $\langle \mathbf{C}_{i,1}, \mathbf{C}_{i,2}, \mathbf{C}_{i,3} \rangle$. These triangles are tangent to the spline surface at the vertices $\mathbf{V}_i$. The projection of a control triangle onto the (x,y)-plane is simply the corresponding PS triangle. Using these control triangles, a

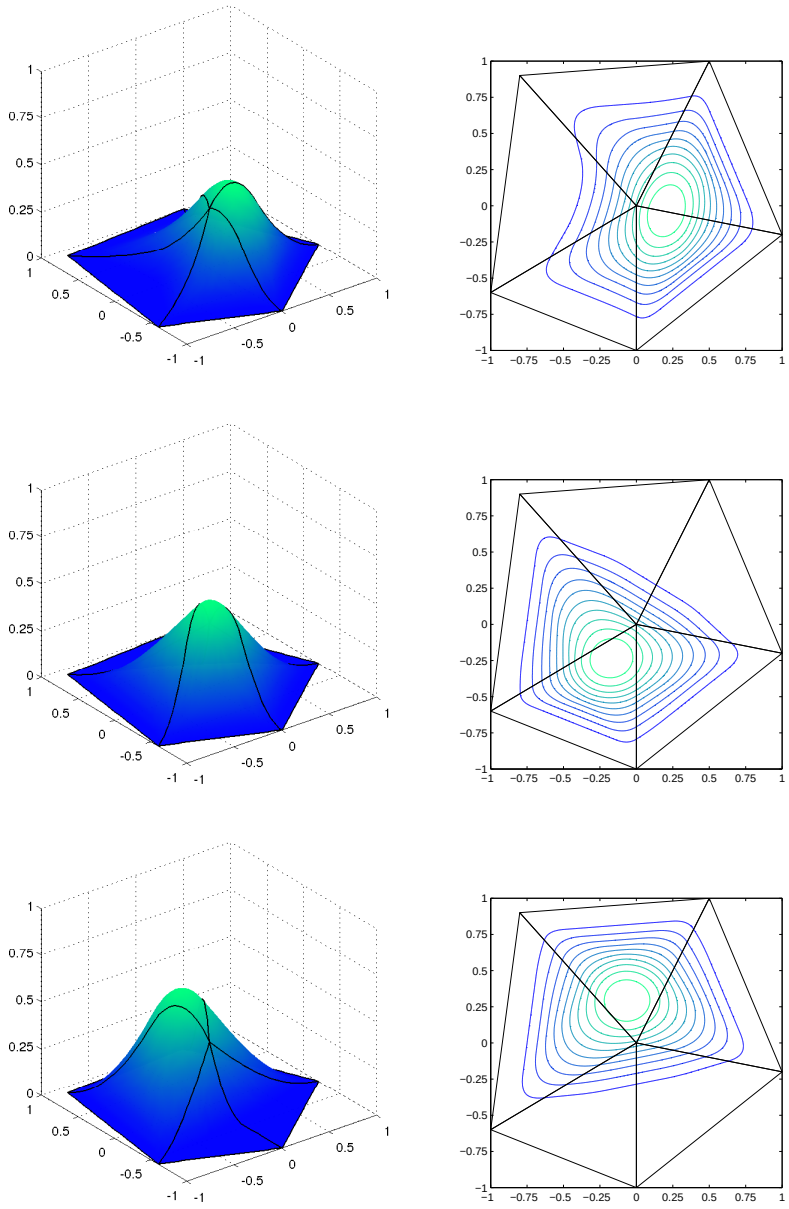

Fig. 32 The three PS B-splines $B_{i,j,\mathcal{T}^*}$, $j=1,2,3$, associated with the vertex $\mathbf{V}_i$ and the PS triangle in Figure 31. Left: the functions $B_{i,j,\mathcal{T}^*}$. Right: the contour lines of $B_{i,j,\mathcal{T}^*}$.

designer can interactively change the shape of a given Powell-Sabin spline locally in a predictable way. The positivity and partition of unity properties guarantee that the graph of the spline (69) lies inside the convex hull of its control points $\mathbf{C}_{i,j}$.

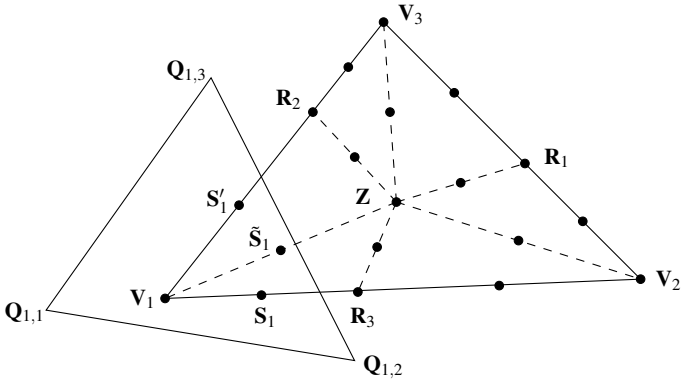

Fig. 33 PS refinement of a reference triangle $T := \langle \mathbf{V}_1, \mathbf{V}_2, \mathbf{V}_3 \rangle$, together with the PS triangle $\mathfrak{T}_1 := \langle \mathbf{Q}_{1,1}, \mathbf{Q}_{1,2}, \mathbf{Q}_{1,3} \rangle$ associated with the vertex $\mathbf{V}_1$

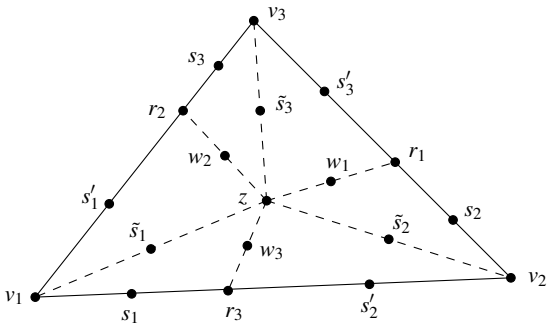

Fig. 34 Schematic representation of the Bézier ordinates of a Powell-Sabin spline.

For further manipulation (e.g. evaluation and differentiation) of a Powell-Sabin spline in the form (69), we can write the spline in a Bézier-Bernstein representation (**Bézier extraction**). We consider a reference triangle $T := \langle \mathbf{V}_1, \mathbf{V}_2, \mathbf{V}_3 \rangle$ with its PS refinement, as shown in Figure 33. All triangles in $\mathcal{T}$ can be treated in this way. We assume that the points indicated in the figure have the following barycentric coordinates:

$$\mathbf{V}_1(1,0,0), \quad \mathbf{V}_2(0,1,0), \quad \mathbf{V}_3(0,0,1), \quad \mathbf{Z}(\zeta_1,\zeta_2,\zeta_3),$$
$$\mathbf{R}_1(0,\rho_1,1-\rho_1), \quad \mathbf{R}_2(1-\rho_2,0,\rho_2), \quad \mathbf{R}_3(\rho_3,1-\rho_3,0).$$

On each of the six subtriangles in T the Powell-Sabin spline is a quadratic polynomial, that can be represented in its Bézier-Bernstein formulation, i.e., with $p=2$ in equations (44) and (45). The value of the corresponding Bézier ordinates is derived in [13]. The outcome is schematically represented in Figure 34, with

$$\begin{aligned} v_1 &= \alpha_{1,1}\,c_{1,1} + \alpha_{1,2}\,c_{1,2} + \alpha_{1,3}\,c_{1,3},\\ s_1 &= \sigma_{1,1}\,c_{1,1} + \sigma_{1,2}\,c_{1,2} + \sigma_{1,3}\,c_{1,3},\\ s'_1 &= \sigma'_{1,1}\,c_{1,1} + \sigma'_{1,2}\,c_{i,2} + \sigma'_{1,3}\,c_{1,3},\\ \tilde{s}_1 &= \widetilde{\sigma}_{1,1}\,c_{1,1} + \widetilde{\sigma}_{1,2}\,c_{1,2} + \widetilde{\sigma}_{1,3}\,c_{1,3}. \end{aligned}$$

Like $(\alpha_{1,1},\alpha_{1,2},\alpha_{1,3})$ are the barycentric coordinates of the vertex $\mathbf{V}_1$, the triplets $(\sigma_{1,1},\sigma_{1,2},\sigma_{1,3})$, $(\sigma'_{1,1},\sigma'_{1,2},\sigma'_{1,3})$ and $(\widetilde{\sigma}_{1,1},\widetilde{\sigma}_{1,2},\widetilde{\sigma}_{1,3})$ are found as the barycentric coordinates of the PS points $\mathbf{S}_1$, $\mathbf{S}'_1$ and $\tilde{\mathbf{S}}_1$, respectively, with respect to the PS triangle $\mathfrak{T}_1$. These points are depicted in Figure 33. Analogously, we can compute the values of $(v_2,s_2,s'_2,\tilde{s}_2)$ and $(v_3,s_3,s'_3,\tilde{s}_3)$. The other Bézier ordinates are derived from the inherent continuity conditions of the Powell-Sabin spline, e.g.,

$$\begin{aligned} r_3 &= \rho_3\,s_1 + (1-\rho_3)\,s'_2,\\ w_3 &= \rho_3\,\tilde{s}_1 + (1-\rho_3)\,\tilde{s}_2,\\ z &= \zeta_1\,\tilde{s}_1 + \zeta_2\,\tilde{s}_2 + \zeta_3\,\tilde{s}_3. \end{aligned}$$

In this Bézier-Bernstein representation the Powell-Sabin spline can be easily manipulated using the de Casteljau algorithm, see (60) with $p=2$.

Being equipped with a B-spline like basis, PS splines admit a straightforward rational extension.

Definition 13. A **NURPS (Non-Uniform Rational PS) surface** on a PS refinement $\mathcal{T}^*$ of a triangulation $\mathcal{T}$ of Ω is defined as

$$\mathcal{S}(\mathbf{X}) = \sum_{i=1}^{N_v}\sum_{j=1}^{3} \mathbf{C}_{i,j} R_{i,j,\mathcal{T}^*}(\mathbf{X}), \quad R_{i,j,\mathcal{T}^*}(\mathbf{X}) := \frac{w_{i,j} B_{i,j,\mathcal{T}^*}(\mathbf{X})}{\sum_{l=1}^{N_v}\sum_{r=1}^{3} w_{l,r} B_{l,r,\mathcal{T}^*}(\mathbf{X})}, \tag{74}$$

where $\mathbf{C}_{i,j}\in\mathbb{R}^d$ are called **NURPS control points**, $B_{i,j,\mathcal{T}^*}$ are the normalized PS B-splines, and $w_{i,j}$ are positive weights.

With particular choices for the control points and weights, NURPS can exactly represent patches on quadric surfaces. The influence of the weights on a NURPS surface can be described in a geometrically intuitive way [40].

As for classical NURBS, see (34), it is sometimes useful to consider the so-called homogeneous representation of (74), in which the NURPS surface is decoupled into $d+1$ standard PS spline components, i.e.

$$\left(\sum_{i=1}^{N_v} \sum_{j=1}^{3} \mathbf{C}_{i,j} w_{i,j} B_{i,j,\mathcal{T}^*}(\mathbf{X}),\ \sum_{i=1}^{N_v} \sum_{j=1}^{3} w_{i,j} B_{i,j,\mathcal{T}^*}(\mathbf{X}) \right). \tag{75}$$

Remark 17. NURPS surfaces can be represented in a Bézier-Bernstein formulation by means of rational Bézier ordinates [42]. They can then be evaluated and manipulated in a stable way by using the rational de Casteljau algorithm.

References

1. Ando, T.: Totally positive matrices. *Linear Algebra Appl.* **90**, 165–219 (1987)
2. Bosner, T., Rogina, M.: Non-uniform exponential tension splines. *Numer. Algor.* **46**, 265–294 (2007)
3. Böhm, W.: A survey of curve and surface methods in CAGD. *Comput. Aided Geom. Design* **1**, 1–60 (1984)
4. Dahmen, W., Micchelli, C. A., Seidel, H.-P.: Blossoming begets B-splines built better by B-patches. *Math. Comp.* **59**, 97–115 (1992)
5. de Boor, C., Höllig, K., Riemenschneider, S.: Box splines. Springer-Verlag (1993)
6. de Boor, C.: A Practical Guide to Splines. Springer, Revised edition (2001)
7. de Boor, C., Pinkus, A.: The approximation of a totally positive band matrix by a strictly banded totally positive one. *Linear Algebra Appl.* **42**, 81–98 (1982)
8. Carnicer, J. M., Peña, J. M.: Shape preserving representations and optimality of the Bernstein basis. *Adv. Comp. Math.* **1**, 173–196 (1993)
9. Carnicer, J. M., Peña, J. M.: Totally positive bases for shape preserving curve design and optimality of B-splines. *Comput. Aided Geom. Design* **6**, 633–654 (1994)
10. Carnicer, J. M., Peña, J. M.: Totally positivity and optimal bases. In: Gasca, M., Micchelli, C. A. (eds.), Total Positivity and its Applications, pp. 133–155. Kluwer, Dordrecht (1996)
11. Cohen, E., Lyche, T., Riesenfeld, R.: Discrete B-splines and subdivision techniques in computer-aided geometric design and computer graphics. *Comput. Graph. Image Process.* **14**, 87–111 (1980)
12. Costantini, P., Lyche, T., Manni, C.: On a class of weak Tchebycheff systems. *Numer. Math.* **101**, 333–354 (2005)
13. Dierckx, P.: On calculating normalized Powell-Sabin B-splines. *Comput. Aided Geom. Design* **15**, 61–78 (1997)
14. Dyn, N., Levin, D.: Subdivision schemes in geometric modelling. *Acta Numer.* **11**, 73–144 (2002)
15. Dyn, N., Levin, D., Luzzatto, A.: Exponentials reproducing subdivision schemes. *Found. Comput. Math.* **3**, 187–206 (2003)
16. Farouki, R. T.: The Bernstein polynomial basis: a centennial retrospective. *Comput. Aided Geom. Design* **29**, 379–419 (2012)
17. Farouki, R. T., Goodman, T. N. T.: On the optimal stability of the Bernstein basis. *Math. Comp.* **65**, 1553–1566 (1996)
18. Gasca, M., Micchelli, C. A. (eds.): Total Positivity and its Applications. Kluwer, Dordrecht (1996)
19. Gasca, M., Peña, J. M.: On the characterization of totally positive matrices In: Singh, S. P. (ed.), Approximation Theory, spline functions and applications, pp. 357–364. Kluwer Academic Publishers, Dordrecht (1992)
20. Goodman, T. N. T., Mazure, M. L.: Blossoming beyond extended Chebyshev spaces. *J. Approx. Theory* **109**, 48–81 (2001)
21. Hoschek, J., Lasser, D.: Fundamentals of Computer Aided Geometric Design. A K Peters (1993)

22. Karlin, S.: Total Positivity. Stanford University Press, Stanford (1968)
23. Koch, P. E., Lyche, T.: Interpolation with exponential B-splines in tension. In: Farin, G., Hagen, H., Noltemeier, H., Knödel, W. (eds.), Geometric modelling, pp. 173–190. Springer-Verlag, London (1993)
24. Kvasov, B., Sattayatham, P.: GB-splines of arbitrary order. *J. Comput. Appl. Math.* **104**, 63–88 (1999)
25. Lai, M.-J., Schumaker, L. L.: Spline Functions on Triangulations. Cambridge U. P. (2007)
26. Lyche, T.: A recurrence relation for Chebyshevian B-splines. *Constr. Approx.* **1**, 155–173 (1985)
27. Mainar, E., Peña, J. M.: A general class of Bernstein-like bases. *Comput. Math. Appl.* **53**, 1686–1703 (2007)
28. MATLAB: Spline Toolbox
29. Mazure, M. L.: Chebyshev-Bernstein bases. *Comput. Aided Geom. Design* **16**, 649–669 (1999)
30. Mazure, M. L.: Chebyshev splines beyond total positivity. *Adv. Comp. Math.* **14**, 129–156 (2001)
31. Mazure, M. L.: How to build all Chebyshevian spline spaces good for geometric design? *Numer. Math.* **119**, 517–556 (2011)
32. Neamtu, N.: What is the natural generalization of univariate splines to higher dimensions? In: Lyche, T., Schumaker, L. L. (eds.), Mathematical Methods for Curves and Surfaces, pp. 355–392. Vanderbilt University Press, Nashville (2001)
33. Neamtu, N.: Delaunay configurations and multivariate splines: A generalization of a result of B. N. Delaunay. *Trans. Amer. Math. Soc.* **359**, 2993–3004 (2007)
34. Peña, J. M. (ed.): Shape Preserving Representations in Computer-Aided Geometric Design. Nova Science Publishers, New York (1999)
35. Powell, M. J. D., Sabin, M. A.: Piecewise quadratic approximations on triangles. *ACM Trans. Math. Software* **3**, 316–325 (1977)
36. Piegl, L., Tiller, W.: The NURBS Book (Monographs in Visual Communication), 2nd edition. Springer-Verlag, New York (1997)
37. Prautzsch, H., Boehem, W., Paluszny, M.: Bézier and B-spline Techniques. Springer (2002)
38. Ramshaw, L.: Blossoms are polar forms. *Comput. Aided Geom. Design* **6**, 323–358 (1989)
39. Schumaker, L. L.: Spline Functions: Basic Theory, third edition. Cambridge U. P. (2007)
40. Speleers, H., Dierckx, P., Vandewalle S.: Weight control for modelling with NURPS surfaces. *Comput. Aided Geom. Design* **24**, 179–186 (2007)
41. Wang, G., Fang, M.: Unified and extended form of three types of splines. *J. Comput. Appl. Math.* **216**, 498–508 (2008)
42. Windmolders, J., Dierckx, P.: From PS-splines to NURPS. In: Cohen, A., Rabut, C., Schumaker, L. L. (eds.), Proceedings of Curve and Surface Fitting, Saint-Malo, 1999, pp. 45–54. Vanderbilt University Press, (2000)
43. Zhang, J., Krause, F., Zhang, H.: Unifying C-curves and H-curves by extending the calculation to complex numbers. *Comput. Aided Geom. Design* **22**, 865–883 (2005)